Title
FOURIER ANALYSIS AND NUMERICAL INTEGRATION; A STEP TOWARDS INVARIANCE GROUP ANALYSIS OF NUMERICAL APPROXIMATIONS

Author
Zingher, Arthur R.

Publication Date
1976-08-01

Submitted to Mathematics of Computation

LBL-5507
Preprint c.1

FOURIER ANALYSIS AND NUMERICAL INTEGRATION; A STEP TOWARDS INVARIANCE GROUP ANALYSIS OF NUMERICAL APPROXIMATIONS

Arthur R. Zingher

August 19, 1976

Prepared for the U. S. Energy Research and Development Administration under Contract W-7405-ENG-48

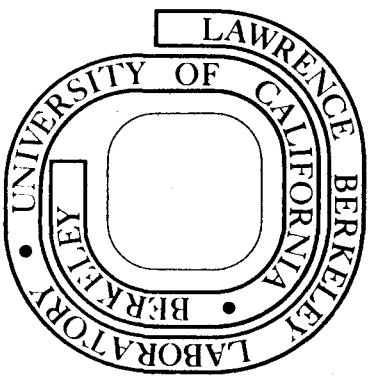

DISCLAIMER

Fourier Analysis and Numerical Integration; A Step Towards Invariance Group Analysis of Numerical Approximations*

by Arthur R. Zingher

Lawrence Berkeley Laboratory
University of California
Berkeley, California 94720

19 August 1976

ABSTRACT. Integration $\int_{-\infty}^{+\infty} dx\ G(x)$ is invariant under the translation $G(x) \to G(x+y)$. We will study the effect of this translation group on the numerical integration $\Sigma_{k=-\infty}^{+\infty} hG(kh)$. This generates a class of equivalent numerical integrations $\Sigma_{k=-\infty}^{+\infty} hG(kh+y)$. This class has simpler invariance group properties than any one approximation alone. This invariance will force us to Fourier analyze the numerical integration. We will extend these results to integration on a finite domain. Often this Fourier analysis will be more

---

*This work was done with support from the U.S. Energy Research and Development Administration.

AMS(MOS) Subject classifications (1970).
Primary 65D30 (Numerical integration)
42A08 (Approximation by trigonometric polynomials)
42A12 (Trigonometric interpolation)

Secondary 81A78 (Physically motivated group representations)
65B15 (Euler-Maclaurin Formula)

Key words and phrases:
Numerical integration, Fourier analysis, invariance group, invariant approximation, numerical analysis, group representations, Nyquist's theorem, Simpson's rule, Gauss-Gregory rule, band-limited functions.

convenient than the polynomial and higher derivative methods of classical numerical analysis. This new analysis will allow us to use many suggestive ideas from communication theory. We will be able to understand a great deal about the errors in numerical integration from ideas of "aliasing" (Nyquist's theorem), the uncertainty principle, and extrapolation. Often the numerical integration error is dominated by needless errors due to implicit extrapolation near the ends of the integration domain. This gives a new insight into the peculiarities of Simpson's rule. This intuition will guide us to strikingly better numerical integration rules which will use samples outside the integration domain. The most exciting consequence is that these ideas are relevant to many numerical analysis problems, not only numerical integration. This is one step on a promising bridge between group theory and numerical analysis.

INTRODUCTION. This paper is the result of a mathematical surprise during the analysis of some hardware. I wanted to count the ions in an intense beam of very fast moving ions. The usual method is to run the beam through a "scintillator," a special plastic which produces a brief light flash when each ion penetrates it. These flashes are then counted photo-electrically. Unfortunately, the ions came faster than the electronics could reliably count.

William Holley, of Lawrence Berkeley Laboratory, suggested a better method: Take a large piece of insensitive plastic and embed many small, equal-sized pieces of scintillator at regular intervals. Then, put this perpendicular to the beam. The regular grid of small scintillators will sample the beam and produce flashes for a constant fraction of the ions. Thus the electronics is not overwhelmed, and can effectively count a very intense beam.

One crucial question was the error due to this spatial sampling. I did not know the beam intensity in detail, but a plausible estimate was a Gaussian, $\exp(-t^2/a^2)$, where t was the position across the beam. The sampling scintillator took samples at intervals $\Delta t=h=a/4$. Thus the exact beam and the sampled beam could be represented as an exact integral and a numerical integral:

$$\int_{-\infty}^{+\infty} dt\ e^{-t^2/a^2} \approx \sum_{k=-\infty}^{+\infty} h\ e^{-(kh)^2/a^2} \quad .$$

How accurately could I expect this coarse numerical integral to approach the exact integral $\sqrt{\pi}$? The result is astounding! On an HP55 the sum is 1.772,453,852. This is identical to $\sqrt{\pi}$ to the 9-figure precision of the calculator!

The application forced me to realize that there are other equivalent calculations. First, the beam occasionally shifted sideways. Second, the scintillator assembly could also shift sideways. Thus an equally plausible equation was

$$\int_{-\infty}^{+\infty} dt\ e^{-(t+y)^2/a^2} \approx \sum_{k=-\infty}^{+\infty} h\ e^{-(kh+y)^2/a^2} \qquad \text{for } y=a/8 \ .$$

The exact integral is invariant under this translation, but the numerical integral is different. Nevertheless, the sum is 1.772,453,851, which is again astoundingly accurate for such a coarse sampling grid.

The exact integral is invariant under the group of translations of the integrand. Therefore it can be approximated by an ensemble of equivalent numerical integrations, which differ only in the fine alignment of their samples. This is the central, new idea in this paper. It is explored graphically in Figs. 1 and 2.

NUMERICAL INTEGRATION ON AN INFINITE DOMAIN. We start by calculating the error in numerical integration over the entire real line. Assume that the integrand G(t) is a complex function, defined on the entire real line, and square-integrable. Consider the rectangular numerical integration rule which adds equally weighted samples G(t) on a uniform grid t = kh+y for all integers k.

$$NI(G;y) \equiv \sum_{k=-\infty}^{+\infty} h\ G(kh+y) \qquad\qquad INT(G) \equiv \int_{-\infty}^{+\infty} dt\ G(t)\ .$$

Notice that the numerical integral depends on an alignment parameter y. This y dependence has three striking properties. First, NI(G;y) is periodic in y with period h.

$$NI(G;y+h) = \sum_{k=-\infty}^{+\infty} h\ G(kh+y+h) = \sum_{k=-\infty}^{+\infty} h\ G([k+1]h+y) = \sum_{k'=-\infty}^{+\infty} h\ G(k'h+y)\ .$$

Second, the mean value of NI(G;y), averaged over a period of y, equals the exact integral.

$$\langle NI(G)\rangle \equiv \frac{1}{h}\int_{o}^{h} dy\ NI(G;y) = \sum_{k=-\infty}^{+\infty} \frac{h}{h}\int_{o}^{h} dy\ G(y+kh)$$
$$= \sum_{k=-\infty}^{+\infty} \int_{kh}^{kh+h} dt\ G(t) = \int_{-\infty}^{+\infty} dt\ G(t)\ .$$

Third, there are at least two values of y that make the numerical integral exact:

$$NI(G;y_{BEST}) = INT(G)\ .$$

Of course, y_{BEST} depends on G.

The periodicity in y strongly suggests using Fourier series analysis with respect to y. We expand NI(G;y) in the Fourier series:

$$NI(G;y) = \sum_{m=-\infty}^{+\infty} \frac{1}{h}\,\tilde{NI}(G;f)\ e^{-i2\pi f_m t} \qquad \text{where } f_m = m/h,$$

where, of course, the coefficients are given by

$$\tilde{NI}(G;f_m) \equiv \int_{o}^{h} dy\ NI(G;y)\ e^{+i2\pi f_m t}\ .$$

Next, we need to Fourier analyze G(t). Since it is not periodic but rather is square-integrable, we must use the Fourier integral:

$$G(t) = \int_{-\infty}^{+\infty} df\ \tilde{G}(t)\ e^{-i2\pi ft}$$

with the inverse

$$\tilde{G}(f) \equiv \int_{-\infty}^{+\infty} dt\ G(t)\ e^{+i2\pi ft} \ .$$

Clearly, $\tilde{NI}(G;f_m)$ should be related to $\tilde{G}(f)$. Unfortunately $\tilde{NI}$ is a function of a discrete variable $f_m=m/h$, and $\tilde{G}$ is a function of a continuous variable f. It requires a little sophistication to connect them rigorously [2]. We use the language of distribution theory, or, equivalently, the language of linear operators over complex square-integrable functions. Some convergence questions are discussed in Appendix A.

The numerical integral can be written as a convolution of a sampling distribution and the integrand:

$$NI(G;y) = \int_{-\infty}^{+\infty} dt\ SAMPLE(y-t)\ G(t)$$ where we define

$$SAMPLE(t') = \sum_{k=-\infty}^{+\infty} h\ \delta(kh-t') \ .$$

A significant result is the Fourier transform of the sampling operator [3]:

$$\tilde{SAMPLE}(f) \equiv \sum_{-\infty}^{+\infty} dt'\ SAMPLE(t')\ e^{+i2\pi ft'} = \sum_{m=-\infty}^{+\infty} \delta(f-m/h) \ .$$

Although SAMPLE(t′) and $\tilde{SAMPLE}(f)$ look similar, nevertheless they are distinct.

The Fourier convolution theorem states that the Fourier transform of the convolution of two functions is the product of the Fourier transforms of the two functions. Therefore,

$$\tilde{NI}(G;f) = \tilde{SAMPLE}(f)\ \tilde{G}(f) = \sum_{m=-\infty}^{+\infty} \delta(f-m/h)\ \tilde{G}(m/h) \ .$$

The error of numerical integration is defined to be the difference between the numerical integral and the exact integral:

$$\mathrm{ERR}(G;y) \equiv \mathrm{NI}(G;y) - \mathrm{INT}(G) \ .$$

The exact integral INT(G) is precisely the zero frequency Fourier transform $\tilde{G}(0)$. Therefore

$$\mathrm{ERR}(G;y) = \int_{-\infty}^{+\infty} df\ \widetilde{\mathrm{SAMPLE}}(G;f)\ e^{-i2\pi fy} - \tilde{G}(0)$$

$$= \sum_{m\neq 0} \tilde{G}(m/h)\ e^{-i2\pi my/h} \ .$$

For many applications, $\tilde{G}(m/h)$ may be known well enough to make this sum useful. For example, sometimes only a few frequencies dominate the sum.

If the magnitude of $\tilde{G}(f)$ is known, but not its phase, then we can still give an upper bound. Use the triangular inequality:

$$\therefore\ |\mathrm{ERR}(G;y)| \leq \sum_{m\neq 0} |\tilde{G}(m/h)| \ .$$

The error will reach this limit only if all terms have the same phase. If G(t) is positive and decreases monotonically away from t=0, then ERR(G;0) will reach the limit. However, if $\{\tilde{G}(m/h)\}$ are not all in phase, then this sum overestimates the error. For example, if G(x) is discontinuous, then the sum diverges.

A more convenient norm for error analysis is often the mean square error, averaged over y. This is estimated by Parseval's equality:

$$||\mathrm{ERR}(G)||^2 \equiv \frac{1}{h}\int_0^h dy\ |\mathrm{ERR}(G;y)|^2$$

$$= \sum_{m_1\neq 0}\ \sum_{m_2\neq 0} \tilde{G}^*(m_1/h)\ G(m_2/h)\ \frac{1}{h}\int_0^h dy\ e^{+i2\pi m_1 y/h}\ e^{-i2\pi m_2 y/h}$$

$$= \sum_{m_1\neq 0}\ \sum_{m_2\neq 0} \tilde{G}^*(m_1/h)\ G(m_2/h)\ \delta(m_1-m_2)$$

$$\therefore\ ||\mathrm{ERR}\ (G)||^2 = \sum_{m\neq 0} |\tilde{G}(m/h)|^2 \ .$$

These results can be interpreted with ideas from communication theory. Since we sample G(t) at regular intervals $\Delta t=h$, we can accurately measure components in $\tilde{G}(f)$ up to a maximum frequency $|f| \leq 1/2h$. We will call an integrand band limited to f_{max} iff its amplitudes $\tilde{G}(f)$ are zero for frequencies $|f| \geq f_{max}$. Nyquist's theorem states that errors will not occur if G is band limited to $f_{max} \leq 1/2h$. Higher frequency components are mismeasured and produce errors. On our regular grid of samples, a higher frequency component has the same values as a lower frequency component.

$$e^{i2\pi f(y+kh)} = e^{i2\pi(f+m/h)(y+kh)} .$$

This misidentification is called "aliasing" [2].

Even though G(t) is not periodic, the regular sampling process makes ERR(G;y) periodic. Since it is linear in $\tilde{G}$, ERR filters the continuous Fourier integral $\tilde{G}(f)$ and passes only the discrete Fourier series $\tilde{G}(m/h)$. Since these components are orthognal under the L^2 inner product, they contribute separately to $||ERR(G)||^2$ without cross-terms.

For a usefully large class of applications an approximate Fourier transform is sufficiently well known to make this a practical error estimate. A very important case is when the step size h becomes very small. Then only the high frequency power spectrum, $|\tilde{G}(f)|^2$ for $|f| \geq 1/h$, is necessary. This high frequency spectrum may be sufficiently well known even if the low and intermediate frequency spectrum is not known.

These Fourier estimates are often particularly convenient to describe properties of experimentally measured data. First and foremost, the hardware often is a low pass filter and removes high frequency components from the experimentally observed samples. Second, a new generation of spectrum analyzers is now available to measure efficiently the approximate Fourier transform of the data. Third, the recent development of the Fast Fourier Transform makes

digital Fourier analysis practical. These hardware developments enable parallel developments in numerical analysis.

INTERPRETATIONS. Hamming introduces the beautiful idea of an invariant algorithm [1.,p.7,72]. We can interpret the preceding analysis with an extension of this idea. The exact integral is invariant under the group of translations of the integrand:

$$\int_{-\infty}^{+\infty} dt\ G(t) = \int_{-\infty}^{+\infty} dt\ G(t+y) \qquad \text{for all real } y.$$

An individual numerical integral NI(G;y) approximates this invariance by being periodic in y, but the exact integral is invariant for all real y. However, the ensemble {NI(G;y) | all real y} is manifestly invariant. The ensemble can be analyzed into irreducible representations of the group. These representations of the translation group are the Fourier basis functions {exp(-i2πft) | for all real f}.

This suggests a generalization. Suppose that an exact calculation is invariant under a group. The elements of this group shall be called symmetries of the exact calculation. We would prefer that the numerical approximations have these same symmetries. Unfortunately, many familar and useful algorithms are not invariant. Given two approximations to the same exact calculation, they will be called equivalent under the group iff a symmetry of the exact calculation transforms one approximation to the other.

An invariant algorithm is an equivalence class of one element. Given an algorithm which is not invariant, it generates an ensemble which is invariant: the set of all equivalent algorithms. Since this ensemble is more symmetric than an individual algorithm, the ensemble should be easier to analyze than an individual algorithm. Group theory provides several tools for this analysis.

Call an algorithm correct under a symmetry group iff it is equivalent to an algorithm which gives the same result as the exact calculation. I speculate that if an algorithm is correct, then its error can be fully described by the group properties. This was the case for numerical integration.

Notice that these generalizations relate to any group of symmetries of an exact calculation. This group need not be the largest possible group, all the symmetries which leave the exact calculation unchanged. This is good. Often we know a few symmetries, but do not know all the symmetries.

Correctness implies that the symmetry will depend on the approximation, as well as the exact calculation. For example, the integration $\int_{-\infty}^{+\infty} dt\ G(t)$ has many symmetries:

$$\underset{\text{TRANSLATION}}{G(t) \to G(t+y)} \qquad \underset{\text{SCALING}}{G(t) \to cG(t/c)} \qquad \underset{\text{REFLECTION}}{G(t) \to G(-t)} \ .$$

Numerical integration is correct with respect to translation, but not scaling nor reflection. However, it would be premature to assume that these other symmetries had no relevance. For example, the scaling group might be a useful tool to study the effect of changing the sampling interval h. We might use scaling alone, or use the group generated by scaling and translation together. Also, the scaling group is related to classical polynomial numerical analysis.

Sometimes the symmetry group gives a lot of information about the exact calculation. For example, the only translationally invariant linear functionals over the space of continuous integrands are integration over $(-\infty, +\infty)$ multiplied by an overall constant.

Quantum mechanics [4] uses group theory in ways which may inspire future work. It describes a physical system by a differential equation. Many important physical systems have significant symmetries. Quantum mechanics translates these physical symmetries into invariance groups of the differential equation. The solutions of these equations are analyzed into

irreducible representations of the invariance group. Also in classical mechanics, there is an important connection between constants of motion and symmetries.

The connection between physical symmetries and computational symmetries is often much stronger than a mathematical analogy. Many numerical analysis problems describe physical systems. Computational symmetries often are a reflection of a symmetry of the original physical system, and not just a mathematical artifice. Conversely, if an applied mathematician finds a symmetry in a mathematical model, then he would be wise to ask what the symmetry means for the original system. For example, the periodicity of the numerical integral NI(G;y) is a discrete translational symmetry. In the hardware described in the Introduction, this symmetry reflected the sideways motion of the beam, and the arbitrary alignment of the sampling scintillator.

Notice that these group theory ideas are not restricted to numerical integration. They should apply to many numerical analysis problems. Of course the relevant symmetries and representations will depend on the specific application.

All this suggests many interesting subsequent papers; but for this one we will continue with the analysis of numerical integration rules. We shall find enough interesting results to justify the steady work.

INFINITE DOMAIN EXAMPLES. The first example dramatizes the difference between Fourier error analysis and classical polynomial numerical analysis. Return to the problem of numerically integrating a Gaussian by the rectangular rule:

$$\begin{aligned} \text{GAUSS}(t) &\equiv \exp(-t^2/a^2) \\ \widetilde{\text{GAUSS}}(f) &= a\sqrt{\pi}\,\exp(-\pi^2 f^2 a^2) \\ |\text{ERR}(\text{GAUSS};y)| &\leq a\sqrt{\pi} \sum_{m\neq 0} \exp(-m^2\pi^2 a^2/h^2) \\ &\approx a\sqrt{\pi}\,\exp(-\pi^2 a^2/h^2)\ . \end{aligned}$$

Divide this error by the exact integral $a\sqrt{\pi}$. Suppose the scan is rather coarse $h = a/4$ with only 8 samples in the peak. The fractional root-mean-square error is only $\exp(-16\pi^2/2) \approx 10^{-34}$! A more reasonable scan $h = a/10$ gives an extraordinary accuracy $\exp(-100\pi^2/2) \approx 10^{-214}$! In actual computation, roundoff effects will be much larger.

This extraordinary convergence is the result of the Gaussian integrand. Consider the product of the normalized variance in t multiplied by the normalized variance in f:

$$(\sigma t)^2\ (\sigma f)^2 \equiv \frac{\int dt\ t^2\ |G(t)|^2}{\int dt\ |G(t)|^2} \times \frac{\int dt\ f^2\ |\widetilde{G}(f)|^2}{\int dt\ |\widetilde{G}(f)|^2}\ ,$$

where G is any function such that all the integrals converge. The Gaussian makes this product uniquely small [4]. I speculate that this makes $||\text{ERR}||^2$ uniquely small for some large class of integrands. What should this class be?

How does this Fourier analysis compare to classical numerical analysis? There we approximately fit the sampled integrand with a polynomial and then integrate that polynomial. Classical numerical analysis finds that the rectangular rule exactly integrates linear polynomials. Insofar as higher powers occur, numerical integration errors will occur. These higher powers can be estimated from the higher derivatives of the integrand. This leads to a variety of error estimates. The simplest estimate comes from the mean value theorem:

$$\max_y |ERR(GAUSS;y)| \leq \frac{h^2}{12} \max_t \left|\frac{d^2}{dt^2} GAUSS\right|$$

$$= \frac{h^2}{12a^2} \max_t |-2 + 4t^2/a^2| = \frac{1}{6} (h/a)^2$$

$$= 1/24 \quad \text{if } h=a/4$$

$$= 1/600 \text{ if } h=a/10 .$$

Thus the simplest form of classical numerical analysis greatly overestimates the maximum error for this problem. Conversely, suppose you want to integrate numerically to a specified accuracy. The better Fourier estimate which we have developed would allow you to use a much coarser numerical integration.

This somewhat exaggerates the crudeness of classical numerical analysis. There are other, more sophisticated integration rules with better error estimates. Unfortunately, the corresponding discussion is also more sophisticated, and the reader may choose to skip the next four paragraphs.

The Euler-Maclaurin formula estimates the error for trapazoid rule integration of a finite interval in terms of the higher derivatives at the ends [5].

$$\int_{-L/2}^{+L/2} dt\, G(t) \equiv h[\tfrac{1}{2} G(-L/2) + G(-L/2+h) + \ldots + G(+L/2-h) + \tfrac{1}{2} G(+L/2)]$$
$$+ \sum_{p=1}^{q} \frac{h^{2p}}{(2p)!} b_{2p} [G^{(2p-1)}(+L/2) - G^{(2p-1)}(-L/2)]$$
$$+ \frac{h^{2q+1}}{(2q)!} \int_{-L/2}^{+L/2} dt\, B_{2q}(t)\, G^{(2q)}(t) ,$$

where b_K and $B_K(t)$ are the K^{th} Bernoulli coefficient and Bernoulli function. The usual method is to evaluate a few terms in the sum and to neglect the rest. One can improve the numerical integration by adding several terms as "end corrections" and estimate the error with the next higher order term.

Suppose we reach the numerical integral on $(-\infty,+\infty)$ as the limit of the uncorrected trapezoid rule as $L \to \infty$. Then all the higher derivative terms form the error estimate. If we stop at q=1, then we get

$$\underset{y}{\text{MAX}} \, |\text{ERR}(G;y)| \leq \frac{h^2}{12} \left[\frac{d^2G}{dt^2}(+L/2) - \frac{d^2G}{dt^2}(-L/2)\right]$$

$$\underset{y}{\text{MAX}} \, |\text{ERR}(\text{GAUSS};y)| \leq \frac{h^2}{6} (2 + L^2/a^2) \exp(-L^2/4a^2) \, .$$

If we take the limit $L \to \infty$ then the error bound has the misleading limit of zero. But certainly the error is <u>not</u> zero. The interpretation should be: if h is sufficiently small, then the error goes to zero faster than h^2 times any constant. Unfortunately this analysis does not tell how small is sufficient, so this bound is not very useful for a numerical calculation.

Suppose you are intent on making the classical numerical analysis work! Do you get a more sensible error bound if you use higher derivatives? No — you get a similar null limit proportional to h^{2q}. If you are really determined and try to let $q \to \infty$, then you still have problems because the correction terms form an asympotic series, and not a convergent series. The problem is that you must take two limits $L \to \infty$, $q \to \infty$ and the convergence is not uniform. I think that if you take the joint limit $L \to \infty$, $q \to \infty$ with q/L^2 fixed, then you get a sensible error bound.

What can we conclude from this long and careful labor? For this problem, classical numerical analysis gives a result which is either excessively crude, or else somewhat vacuous, or else very difficult to evaluate. Hamming [1., p. 348] concludes that, in the context of classical numerical analysis of the Gaussian integral,

"The remarkable accuracy for h=1/2 is unfortunately accompanied by a certain lack of knowledge of when it occurs, or when h is too large; the error analysis of Gregory's formula is a difficult topic."

This is not a blanket rejection of classical numerical analysis; rather, it limits them to integrands which have rapidly convergent power series. Conversely, this Fourier error analysis should be efficient only if the Fourier transform $\tilde{G}(f) \to G(t)$ converges quickly.

Our second example will be easier. Suppose the integrand is experimentally determined by a sequence of measurements $G(x_k)$ at a uniform grid of sample locations $x_k = kh+y$ for integer k. Suppose each measurement $G(x_k)$ is a sum of an ideal signal $S(x_k)$ and experimental noise $N(x_k)$. Let $\tilde{S}(f)$ and $\tilde{N}(f)$ be the corresponding Fourier transforms. Suppose the noise is described by a set of representative noises. Let $\langle \ldots \rangle$ indicate an average over this set. Suppose the average noise is zero:

$$\langle N(x) \rangle = 0 \quad \text{and hence} \quad \langle \tilde{N}(f) \rangle = 0 \ .$$

We often know an approximation to the average power spectrum for the noise $\langle |\tilde{N}(f)|^2 \rangle$. From this it is very easy to see what error the noise produces in the numerical integral NI(G;y). A common example is "shot noise" or "pink noise" which falls off at high frequencies.

$$\langle |\tilde{N}(f)|^2 \rangle = g^2 \exp(-\tau|f|) \qquad \text{with g, } \tau \text{ positive.}$$

Here g is characteristic noise size, and $1/\tau$ is a characteristic noise frequency. Then the average square error is

$$\begin{aligned}
\langle ||\mathrm{ERR}(G)||^2 \rangle &= \sum_{m \neq 0} \langle |\tilde{S}(m/h) + N(m/h)|^2 \rangle \\
&= \sum_{m \neq 0} \langle |\tilde{S}(m/h)|^2 \rangle + 2 \langle \mathrm{Re}\ \tilde{S}^*(m/h)\ \tilde{N}(m/h) \rangle + \langle |\tilde{N}(m/h)|^2 \rangle \\
&= \sum_{m \neq 0} |\tilde{S}(m/h)|^2 + 2\ \mathrm{Re}\ \tilde{S}^*(m/h)\ \langle \tilde{N}(m/h) \rangle + g^2 \exp(-|m|\tau/h), \\
\therefore \langle ||\mathrm{ERR}(G)||^2 \rangle &= ||\mathrm{ERR}(S)||^2 + 0 + \frac{2\, g^2 \exp(-\tau/h)}{1 - \exp(-\tau/h)}
\end{aligned}$$

Thus the net mean square error is the sum of an error produced by the signal, and one produced by the noise, and there are no cross terms. If the sampling interval is short compared to the typical noise frequency, then $h \ll \tau$ and the extra squared error is $2g^2\exp(-\tau/h)$. If the sampling interval is long then $h \gg \tau$ and the extra error is $2g^2\, h/\tau$.

This is not the only way to estimate the noise error. Autocorrelation arguments can be used to estimate $\langle | d^2N/dt^2 |^2 \rangle$ and these will lead to corresponding estimates. However, you must use some care, because d^2N/dt^2 may be singular for some representative noises. If sufficient t-domain information is available, then these higher derivative methods may be useful. But in experimental applications, often the noise Fourier spectrum is easier to estimate because of the hardware developments discussed before.

NUMERICAL INTEGRATION ON A FINITE DOMAIN. Here we will develop the corresponding theory for integration on a finite real domain

$$\int_{-L/2}^{+L/2} dt\ G(t)$$

Can we directly use the preceding theory? Assume that G(t) is defined on the entire real line and is square integrable. A first attempt is to truncate the integrand. Let $\mathcal{G}(t) \equiv G(t)\ \mathrm{EXACT}(t)$ where

$$\begin{aligned} \mathrm{EXACT}(t) &\equiv 1 \text{ if } |x| < L/2 \\ &\equiv \tfrac{1}{2} \text{ if } |x| = L/2 \\ &\equiv 0 \text{ if } |x| > L/2\ . \end{aligned}$$

I use the name EXACT because we will see that this is closely related to the exact integral.

Now analyze $\int_{-\infty}^{+\infty} dt\, G(t)$. The preceding theory gives a misleadingly large error estimate. Since EXACT is discontinuous, in general $\tilde{G}(f)$ will have large high frequency components. Conclusion: we must analyze another way.

The solution is suggested by the symmetry group ideas which we developed before. The infinite domain integral INT(G) was invariant under the group of realignments, $G(t) \to G(t+y)$. An individual numerical integral NI(G;y) did not share this symmetry, so we created a symmetric ensemble by considering the class of all realigned numerical integrals. By comparison, the finite domain exact integral is <u>not</u> invariant. But we can construct an invariant ensemble by considering all realigned finite domain exact integrals.

Thus we have an <u>invariant ensemble of exact calculations</u> which parallels the <u>invariant ensemble of approximations</u>.

This idea is developed graphically in Fig. 3. When we change the alignment y, then the numerical integration samples a different domain. We should compare this with a realigned exact integral:

$$\mathrm{INT}(G;y) \equiv \int_{-L/2}^{+L/2} dt\, G(t)$$

$$= \int_{-\infty}^{+\infty} dt\, \mathrm{EXACT}(y-t)\, G(t) \ .$$

Now apply the Fourier convolution theorem:

$$\mathrm{INT}(G;y) = \int_{-\infty}^{+\infty} df\, \tilde{G}(f)\, \tilde{\mathrm{EXACT}}(f)\, e^{-i2\pi fy} \ , \text{ where}$$

$$\tilde{\mathrm{EXACT}}(f) = \int_{-\infty}^{+\infty} dt'\, \mathrm{EXACT}(t')\, e^{+i2\pi ft}$$

$$= \sin(\pi fL)/\pi f \ .$$

We require G(t) to be square-integrable on the entire real line to make $\tilde{G}(f)$ well defined. Also, since INT(G;y) is not periodic, we must use the Fourier integral, $\tilde{G}(f)$ for all real f, and not just the discrete Fourier series $\tilde{G}(m/h)$.

Next, define the numerical integration. Let {WT(n) | integer n} be a set of coefficients, called WeighTs. The Numerical Integration is defined

$$NI(G;y) \equiv \sum_{h=-\infty}^{+\infty} h\ G(y-kh)\ WT(k) \ .$$

The weights implicitly depend on L, and h, and on the numerical integration rule. They cut off the summation for large k to locate the integration domain. This may occur by WT(k) = 0 everywhere outside the integration domain $|kh| \leq L/2$. Or it may include a few non-zero weights just beyond the ends to make end corrections. Or it may even include non-zero weights far beyond the ends, but with sufficiently small weights to make the sum converge. For future convergence it will be sufficient to assume that the weights are absolutely summable:

$$\sum_{k=-\infty}^{+\infty} h\ |WT(k)| < \infty \ .$$

Examples are given in Fig. 4.

The error ERR(G;y) is defined to be the difference between the numerical integral and the exact integral:

$$ERR(G;y) = NI(G;y) - INT(G;y) \ .$$

Since neither integral is a periodic function of the alignment y, this difference need not be periodic. Nevertheless, we can construct its Fourier integral:

$$\tilde{ERR}(G;f) \equiv \int_{-\infty}^{+\infty} dy\ ERR(G;y)\ e^{+i2\pi fy} \ .$$

Now evaluate this transformed error. First rewrite NI and INT as convolutions:

$$NI(G;y) = \int_{-\infty}^{+\infty} dt\ G(t)\ SAMPLEWT(y-t) \text{ , where}$$

$$SAMPLEWT(t') = \sum_{k=-\infty}^{+\infty} h\ \delta(t'-kh)\ WT(k) \text{ , and}$$

$$INT(G;y) \equiv \int_{-\infty}^{+\infty} dt\ EXACT(y-t)\ G(t) \text{ .}$$

Unlike the preceding infinite domain case, the Fourier transform of the sampling operator will converge and not be singular:

$$\widetilde{SAMPLEWT}(f) = \sum_{k=-\infty}^{+\infty} h\ e^{+i2\pi fkh}\ WT(k) \text{ .}$$

Since $\exp(+i2\pi fh) = \exp(+i2\pi\ [f\pm 1/h]\ kh)$, it follows that $\widetilde{SAMPLEWT}(f)$ is periodic in f. This will become significant later.

We can now apply the Fourier convolution theorem. This gives our main result, an exact formula for the numerical integration error:

$$ERR(G;y) = \int_{-\infty}^{+\infty} df\ \widetilde{G}(f)\ \widetilde{E}(f)\ e^{-i2\pi fy} \text{ , where}$$

$$\widetilde{E}(f) = \text{ Fourier Error Coefficient (f)}$$

$$= \widetilde{SAMPLEWT}(f) - \widetilde{EXACT}(f) \text{ .}$$

In the next section we will see that $\widetilde{E}(f)$ is near zero for much of the frequency domain. This will allow us to approximate the error ERR(G;y) using only limited information about $\widetilde{G}(f)$. If we have even less information, and if our application can use a less exact error estimate, then we can make various simplifications. An upper bound follows from the triangular inequality:

$$|ERR(G;y)| \leq \int_{-\infty}^{+\infty} df\ |\widetilde{G}(f)|\ |\widetilde{E}(f)| \text{ .}$$

In other applications, a root mean square average is preferable. Since ERR(G;y) is not periodic, we must construct the average a little differently than before. We define a norm

$$||\mathrm{ERR}(G;y)||^2 \equiv \frac{1}{L}\int_{-\infty}^{+\infty} dy\ |\mathrm{ERR}(G;y)|^2 .$$

Appendix A shows that this converges. Now use Parseval's equality: the mean-square norm with respect to y equals the mean-square norm with respect to f.

$$||\mathrm{ERR}(G)||^2 = \frac{1}{L}\int_{-\infty}^{+\infty} df\ |\mathrm{ERR}(G;f)|^2$$

$$= \int_{-\infty}^{+\infty} df\ |\tilde{G}(f)|^2\ |\tilde{E}(f)|^2/L .$$

In the next section we will study $\tilde{E}(f)$ for several important numerical integration rules. These can be rewritten trivially to calculate $|\tilde{E}(f)|$ or $|\tilde{E}(f)|^2/L$ to study error upper bounds or mean square errors. To repeat, the choice between these depends on the application.

SEVERAL IMPORTANT NUMERICAL INTEGRATION RULES. Now we will study the Fourier error coefficients $\tilde{E}(f)$ for several important numerical integration rules. We will try to concentrate on interpretation and qualitative ideas and will try not to be overwhelmed by the algebra. Nevertheless, the reader must persevere through several difficult pages. In the next section the discussion will become easier, and the reader will be rewarded with some interesting results. Some of the algebraic details have been exiled to Appendix B. Figure 4 is a pictorial catalogue of these numerical integration rules.

Start with the midpoint RECTangular Numerical Integration rules, which has the obvious acronym NIRECT. Assume that the sampling period h divides the integration domain L into 2N, an even integer number of samples. Let $G_k \equiv G(kh+y)$.

$$\text{NIRECT}(G;y) = h[G_{-N+1/2} + G_{-N+3/2} + \ldots + G_{+N-3/2} + G_{+N-1/2}]$$

$$= \int_{-\infty}^{+\infty} dt\ \text{RECT}(y-t)\ G(t), \qquad \text{where the kernel is}$$

$$\text{RECT}(z) = \sum_{k=-N+1/2}^{k=+N-1/2} h\ \delta(kh+z) \qquad \text{whose Fourier transform is}$$

$$\widetilde{\text{RECT}}(f) = \sum_k h\ e^{+i2\pi fkh} = h\ \sin(\pi fL)/\sin(\pi fh)\ .$$

By comparison, the kernel of the exact integral gave $\widetilde{\text{EXACT}}(f) = \sin(\pi fL)/\pi f$. Therefore the Fourier error coefficient is

$$\widetilde{\text{ERECT}}(f) = h\ \sin(\pi fL)/\sin(\pi fh) - \sin(\pi fL)/\pi f\ .$$

Now we work towards getting some insight out of this messy algebra. Start by factoring $\widetilde{\text{RECT}}(f)$ from $\widetilde{\text{ERECT}}(f)$.

$$\widetilde{\text{ERECT}}(f) = \widetilde{\text{RECT}}(f)\ [1 - \sin(\pi fh)/\pi fh]$$

$$\equiv \widetilde{\text{RECT}}(f)\ \widetilde{\text{MODRECT}}(f)\ .$$

These functions are plotted in Fig. 5AB. Start by concentrating on $\widetilde{\text{RECT}}(f)$. This shows a pattern of large spikes superimposed on fine small oscillations. These spikes are due to aliasing, which we already discussed. We will call them Nyquist spikes.

Compare this with the error for integration on the entire real line. The language was somewhat different, but the corresponding Fourier error coefficient was a singular operator

$$\widetilde{\text{SAMPLE}}(f) = \sum_{m\neq 0} \delta(f-m/h)\ .$$

Thus the spikes in $\widetilde{\text{ERECT}}(f)$ approach these delta functionals.

For the finite domain, the Nyquist spikes have width $\Delta f \approx 1/L$ because of the factor $\sin(\pi fL)$ in $\tilde{RECT}(f)$. This width is the result of the uncertainty principle that measurements on a domain of length L cannot determine a frequency more precisely than $\Delta f \approx 1/L$. (This is not the most precise statement of the principle, because that would divert us from our main discussion. The uncertainty principle is well known in physics [4] and communication theory. We skirted it in our study of the Gaussian integrand.) We conclude that $\tilde{RECT}(f)$ summarizes the almost unavoidable errors of any numerical integration method based on a finite density of regularly spaced samples.

There is one exception: zero frequency components are correctly represented by the samples. Consider the other factor in $\tilde{ERECT}(f)$. It is convenient to measure frequency in comparison to the sampling interval $\theta \equiv \pi fh$:

$$\begin{aligned} \text{MOD}\tilde{\text{RECT}}(f) &\equiv 1 - \sin\theta/\theta \\ &\approx \theta^2/6 && \text{if } |\theta| \ll 1 \\ &\approx 1 && \text{if } |\theta| \gg 1 . \end{aligned}$$

This has a double root at zero frequency. This eliminates the zero frequency Nyquist spike and reduces (filters) the errors at low frequencies, $|f| \leq 1/\pi h$.

Now we can study how the error changes as the sample interval is reduced, $h \to 0$. The starting point is our main formula for errors, with the h dependence written out explicitly.

$$\text{ERR-RECT}(G;y;h) = \int_{-\infty}^{+\infty} df\ \tilde{G}(f)\ \tilde{ERECT}(f;h)\ e^{-i2\pi fy}$$

$$\begin{aligned} \tilde{ERECT}(f;h) &= h\ \sin(\pi fL)/\sin(\pi fh) - \sin(\pi fL)/\pi f \\ &= [\pi fh/\sin(\pi fh) - 1]\ \sin(\pi fL)/\pi f . \end{aligned}$$

We already know a great deal about the way the Nyquist spikes change with h. The peak frequency $f_m = m/h$ will scale up, but the width $f \approx 1/L$ and the peak height $ERECT \approx L$, are both independent of h. If G is band limited to f_{max}, then the errors indicated by the Nyquist spikes will disappear for $h \leq 1/f_{max}$. This part of the h dependence is carried by the factor $\widetilde{RECT}(f;h)$ in $\widetilde{ERECT}(f;h)$.

Alternatively, consider one fixed frequency f, and let $h \to 0$. The last formula for $\widetilde{ERECT}(f;h)$ isolates all h dependence into the factor in square brackets. When h becomes small compared to $1/|f|$, then this factor is approximately equal to $(\pi fh)^2/6$. Thus the error coefficient will become small like h^2, once h is sufficiently small. However, "sufficiently small" depends on f, and this convergence is non-uniform in f. This part of the h dependence is carried by the factor $\widetilde{MODRECT}(f;h)$ in $\widetilde{ERECT}(f;h)$.

It would be misleading to conclude that the overall error converges to zero like

$$|\text{ERR-RECT}(G;y;h)| \leq \frac{(\pi h)^2}{6} \int_{-\infty}^{+\infty} df\ |G(f)|\ f^2 \times \sin(\pi fL)/\pi f\ .$$

The first problem is that this upper bound does not follow because the h^2 approximation depends on f. In other words, the error coefficient converges non-uniformly to zero. The second problem is that this upper bound is infinite if G(t) is not everywhere differentiable. Third, and most insidious, this bound may often seriously overestimate the error.

Often the integrand is not only band-limited, but the power spectrum $|\widetilde{G}(f)|^2$ is largest at low frequencies and falls approximately monotonically as the frequency increases in magnitude. In such cases, the main formula for the error is more sensitive to values of $\widetilde{ERECT}(f;h)$ at low frequencies, and less sensitive at high frequencies. The non-uniform convergence means that the low frequency error coefficients will shrink as $h \to 0$ before the

high frequency coefficients start to shrink. Thus the error will shrink before this misleading upper bound would indicate. These problems are similar to the problems we already studied in the example of the second-derivative error bound for the Gaussian integrand. This non-uniform convergence and extra low frequency sensitivity should be kept in mind when we study other numerical integration rules.

The TRAPezoidal rule for Numerical Integration is

$$\text{NITRAP}(G;y) = h[1/2\ G_{-N} + G_{-N+1} + \ldots + G_{+N-1} + 1/2\ G_{+N}] .$$

As before, this can be written as the convolution of G(t) with a kernel TRAP(y-t). Appendix B shows that its Fourier transform is

$$\tilde{\text{TRAP}}(f) \equiv h\ \sin(\pi fL)/\tan(\pi fh) .$$

Therefore its error coefficient is

$$\tilde{\text{ETRAP}}(f) = \tilde{\text{RECT}}(f)\ \tilde{\text{MODTRAP}}(f), \text{ where}$$

$$\tilde{\text{MODTRAP}}(f) \equiv \cos\theta - \sin\theta/\theta$$

$$\approx \theta^2 2/3 \qquad \text{if } |\theta| << 1 .$$

We will interpret this after we have developed other integration rules.

Simpson's rule on the same samples is

$$\text{NISIMP}(G;y) = h[1/3\ G_{-N} + 4/3\ G_{-N+1} + 2/3\ G_{-N+2} + 4/3 + 2/3 + \ldots$$
$$+ 2/3\ G_{+N-2} + 4/3\ G_{+N-1} + 1/3\ G_{+N}] .$$

Appendix B calculates the Fourier transform of its kernel:

$$\tilde{\text{SIMP}}(f) = \{2h\ \sin(\pi fL)\ /\ \sin(2\pi fh)\}\ [1 + 2/3\ \cos(2\pi fh)]$$

$$= \tilde{\text{RECT2H}}(f)\ [1 + 2/3\ \cos(2\theta)] .$$

Notice that $\tilde{\text{SIMP}}(f)$ contains a factor $\tilde{\text{RECT2H}}(f)$ which has the same form as $\tilde{\text{RECT}}(f)$, but with h replaced by 2h. We will interpret this later. The error coefficient $\tilde{\text{ESIMP}}(f)$ contains a corresponding factor. The Fourier error coefficient is

$$\widetilde{ESIMP}(f) = \widetilde{RECT2H}(f)\ \widetilde{MODSIMP}(f), \text{ where}$$

$$\widetilde{MODSIMP}(f) \equiv 2/3 + 1/3\cos(2\theta) - \sin(2\theta)/2\theta$$

$$\approx +.0888\ \theta^4 \qquad \text{if } |\theta| << 1 .$$

We will discuss Simpson's rule further after we evaluate the first order centered Gauss Gregory rule which we abbreviate CGG [6]. This corrects the trapezoidal rule with centered differences at each end. (This correction is similar to the first order Euler-Maclaurin correction to the trapezoidal rule.)

$$NICGG(G;y) \equiv h[-1/24\ G_{-N-1} + 1/2\ G_{-N} + 25/24\ G_{-N+2} + G_{-N+3} + \ldots$$

$$+ G_{+N-3} + G_{+N-2} + 25/24\ G_{+N-1} + 1/2\ G_{+N} - 1/24\ G_{+N+1}] .$$

Appendix B shows that the Fourier error coefficient is

$$\widetilde{ECGG}(f) = \widetilde{RECT}(f)\ \widetilde{MODCGG}(f), \text{ where}$$

$$\widetilde{MODCGG}(f) = \cos\theta + \frac{1}{3}\sin^2\theta - \sin\theta/\theta$$

$$\approx -.0777\ \theta^4 \qquad \text{if } |\theta| << 1 .$$

GRAPHICAL COMPARISONS AND INTERPRETATIONS. These Fourier coefficients can most easily be compared graphically. They have been evaluated and plotted with a simple FORTRAN program for the errors of numerical integration of

$$\int_{-10}^{+10} dt\ G(t), \text{ where } h = 1.$$

Since $\widetilde{ERECT}(f)$ is a common factor in all but one rule, we can compare the error coefficients by just comparing their modulations. Figure 6A shows the low and intermediate frequency bands $|f| \leq 0.9$ cycle/sample. Notice that $\widetilde{MODRECT}(f)$ and $\widetilde{MODTRAP}(f)$ are both approximately parabolic, with the trapezoidal errors about twice the rectangular errors. The other rules $\widetilde{MODSIMP}(f)$ and $\widetilde{MODCGG}(f)$ are almost identical quartics. Figure 6B shows the individual modulations up to high frequencies $|f| \leq 3$ cycles/sample, and Fig. 6C superimposes them. This last figure is complex, with many overlapping

curves. The important feature is that all the rules have comparable magnitude in the high frequency band, $|f| \geq 1$ cycle/sample. All are on the order of one. Therefore, they will produce similar errors in this band.

Simpson's rule needs some interesting special consideration. Recall that its Fourier error coefficient has a factor $\widetilde{\text{RECT2H}}(f)$ instead of $\widetilde{\text{RECT}}(f)$. This requires that we compare the error coefficients $\widetilde{\text{ESIMP}}(f)$, Fig. 7A, and $\widetilde{\text{ECGG}}(f)$, Fig. 7B. At low frequencies, $|f| \leq 1/3$ cycle/sample, these errors are very similar. At intermediate frequencies, $|f| = 1/3$ to 1 cycle/sample, we see that Simpson's rule is much worse! Why? Inspect the weights in Fig. 4 for Simpson's rule. They give little weight to alternate samples. So Simpson's rule approximates CGG with half the density of samples. Therefore Simpson's rule must develop Nyquist spikes at half the frequencies that CGG does. The extra spikes happen to have negative phase and are conspicuous in Fig. 7A.

A more precise statement is possible. The sampling weights for Simpson's rule repeat with sampling period 2h, even though the sampling interval is h. The Nyquist spikes show aliasing errors. These occur at harmonics of the sampling period $f = m/2h$. On the other hand, CGG gives equal weights to all its samples. Thus its sampling period and interval are identical. Therefore its Nyquist spikes are at $f = m/h$. This distinction between the repetition period and the sampling interval is reinforced by the convolution algebra in Appendix B. There the repetition clearly introduces the factors $\widetilde{\text{RECT}}(f)$ and $\widetilde{\text{RECT2H}}(f)$.

This makes Simpson's rule seem very crude. But it is well known to be better than the trapezoidal rule for many integrands. In the low frequency band Simpson's rule is much better than the trapezoidal rule (see Fig. 6A). Why? Because it handles the ends of the integration domain well. The CGG makes this clear. Throughout the bulk of the summation, everywhere except at the ends of the integration domain, CGG is identical to the trapezoidal rule (see Fig. 4). Therefore, they have similar Nyquist spikes, and similar $\widetilde{\text{RECT}}(f)$ factors. But the subtle differences near the ends of the integration domain imply different modulation factors. These determine the low frequency error. There the trapezoidal rule error is proportional to θ^2, while the CGG error is proportional to θ^4.

Why should fine details near the end make such an extraordinary difference in the errors? Aren't these insignificant compared to the many samples inside the integration domain? No! We can think of numerical integration in two stages. First, we construct an approximation to the integrand from the given samples. Second, we calculate the exact integral of this approximation. Well inside the domain, with many samples on each side, the approximation is an <u>interpolation</u> problem. Near an end, with very few samples on one side, the approximation is like an <u>extrapolation</u> problem. Extrapolation is much more difficult than interpolation, and it dominates the errors at low frequencies. Simpson's rule and CGG are better than the trapezoidal rule because they do this extrapolation better. Simpson's rule is <u>not</u> improved because the weights inside the domain alternate in some clever way. Indeed, the Nyquist spike analysis showed that this alternation is a weakness. The improvement is due to better extrapolation near the ends.

A useful concept, due to Tsvi White, is the data domain for a numerical integration rule. This is the set of all locations of the required samples. Compare the data domain and the integration domain. Iff the data domain is inside the integration domain excluding the end points, then that numerical integration rule is open. The midpoint rectangular rule is open since its samples never are closer than h/2 from either end. Call a rule closed iff its data domain is the ends plus locations inside the integration domain. The trapezoidal rule and Simpson's rule are closed. Call a rule extended iff its information domain includes points beyond the ends of the integration domain, as well as inside the integration domain. The CGG rule is extended since the centered difference at each end requires one sample beyond each end. For a given density of samples, the progression from an open rule, to a closed rule, to an extended rule can change the errors associated with the ends from extrapolation errors to interpolation errors.

The natural context for this analysis is integrands with well defined Fourier transforms. Nevertheless, we will briefly consider polynomial integrands because they dominate classical numerical integration. Polynomials can be Fourier transformed within distribution theory. The Fourier transform of a polynomial (of finite degree) vanishes except at very low frequencies:

$$\text{Fourier transform } (x^m;f) = \delta(f)(-2\pi i)^{-m}(\partial/\partial f) \ .$$

Substitute this integrand into our main error formula for $ERR(x^m;y)$. Simpson's rule and CGG have error coefficients like $(hf)^4$ as $hf \to 0$, so it follows that both rules integrate cubic polynomials exactly.

There are many possible comparisons between polynomial and Fourier methods. For low order polynomials ($m \leq L/h$) and low frequencies ($|f| \leq 1/h$) the two methods give very similar results. Beyond this, some integrands are better analyzed by one method, and some by the other. If an integrand has a rapidly

convergent power series, then polynomial methods should work well. If it has a rapidly convergent Fourier transform, then Fourier methods should work well. The tool should fit the task. One cannot say that either method is categorically better.

We conclude this section with several generalizations. First, if extended samples are available, then the centered Gauss-Gregory rule is better than Simpson's rule. Second, every rule with uniformly spaced samples will make aliasing errors, which will produce Nyquist spikes. Third, the best rule should have equal weights inside the integration domain. Near the ends it should be more sophisticated, to alleviate the extrapolation problem; if possible, it should use extended samples to eliminate this problem. In the next section we will develop these ideas to their logical conclusion.

AN OPTIMAL NUMERICAL INTEGRATION RULE. What is the best possible numerical integration rule, as measured by its mean-square error spectrum?

$$||\mathrm{ERR}(G)||^2 = \int_{-\infty}^{+\infty} df\ |\tilde{G}(f)|^2\ |\tilde{E}(f)|^2/L\ .$$

Clearly the answer depends on the integrand's power spectrum $|\tilde{G}(f)|^2$. Insofar as it is known, the rule should be tuned to make the Fourier coefficient coefficient $|\tilde{E}(f)|^2$ small wherever $|\tilde{G}(f)|^2$ is large. How large a set of frequencies can have zero error coefficient? Does any rule reach this optimum?

We need to recall some previous results. Let NI(G;y) be the numerical integration which approximates $\int_{-L/2}^{+L/2} dt\ G(t+y)$ with a regular grid of samples and some unspecified weights:

$$\mathrm{NI}(G;y) \equiv \sum_{k=-\infty}^{+\infty} h\ G(kh+y)\ \mathrm{WT}(k)\ .$$

Assume that L/h is an even integer. We already constructed the Fourier transform of the kernel, $\widetilde{\text{SAMPLEWT}}(f)$, and we saw that it was periodic in f, with period $\Delta f = 1/h$. The error coefficient was the difference between this kernel and the corresponding kernel for the exact integral:

$$\widetilde{E}(f) = \widetilde{\text{SAMPLEWT}}(f) - \widetilde{\text{EXACT}}(f) .$$

Obviously this error will be zero at some particular frequency, if and only if

$$\widetilde{\text{SAMPLEWT}}(f) = \widetilde{\text{EXACT}}(f) \equiv \sin(\pi f L)/\pi f .$$

Now we are prepared to restate the question. Consider all such numerical integrals. Each rule will have a set of roots $\{f | E(f) = 0\}$. What rule gives a maximal set of roots? What periodic functions $\widetilde{\text{SAMPLEWT}}(f)$ have a maximal solution to the following equation?

$$\widetilde{\text{SAMPLEWT}}(f)/\sin(\pi f L) = 1/\pi f .$$

The left-hand side is periodic in f, but the right-hand side never repeats a value. Therefore, if this equation is satisfied for frequency f_1, then it must <u>not</u> be satisfied for frequency $f_1 + m/h$ for any non-zero integer m. Thus all roots are distinct modulo $\Delta f = 1/h$. Therefore a maximal set of roots will be $(-1/2\ h;\ +\ 1/2h]$ if we can find a rule with these roots.

There is one loophole. The preceding argument is not valid if $\sin(\pi f L) = 0$. In that case, the error will be zero if $\widetilde{\text{SAMPLEWT}}(f) = \sin(\pi f L) = 0$. These frequencies generate the functions with period L.

Now we construct a numerical integration rule which is exact up to frequencies 1/2h in magnitude. This sounds like a difficult condition to fulfill, but it turns out to be quite moderate. This condition implies that

$$\widetilde{\text{SAMPLEWT}}(f) = \widetilde{\text{EXACT}}(f) = \sin(\pi f L)/\pi f$$

if f is in the fundamental band $f \in (-1/2\ h;\ +\ 1/2\ h]$.

Define a new function, f modulo 1/h. Let mod(f) be that frequency in the fundamental band which differs from f by an integer multiple of 1/h. Then, since $\widetilde{\text{SAMPLEWT}}(f)$ is periodic, it is determined everywhere by its values for f in the fundamental band. Therefore

$$\widetilde{\text{SAMPLEWT}}(f) = \widetilde{\text{EXACT}}(\text{mod}(f)) = \sin(\pi f L)/\pi \text{ mod}(f) \quad \text{for all } f.$$

We cannot naively take the Fourier transform of $\widetilde{\text{SAMPLEWT}}(f)$ because it is periodic and not square-integrable. This is precisely the same problem which we already overcame to study numerical integration on an infinite domain. There we used a special operator

$$\text{SAMPLE}(t) \equiv \sum_{k=-\infty}^{+\infty} h\ \delta(t-kh) \qquad \text{whose Fourier transform was}$$

$$\widetilde{\text{SAMPLE}}(f) = \sum_{m=-\infty}^{+\infty} \delta(f-m/h) \ .$$

Let $\widetilde{\text{BANDLIMIT}}(f)$ be the characteristic function of the band (-1/2 h; + 1/2 h).

$$\widetilde{\text{BANDLIMIT}}(f) \equiv 1 \quad \text{if } |f| < 1/2\ h$$
$$\equiv 1/2 \quad \text{if } |f| = 1/2\ h$$
$$\equiv 0 \quad \text{if } |f| > 1/2\ h$$

The periodicity of $\widetilde{\text{SAMPLEWT}}(f)$ can now be expressed by the infinite sum

$$\text{SAMPLEWT}(f) = \sum_{m=-\infty}^{+\infty} \widetilde{\text{EXACT}}(f-m/h)\ \widetilde{\text{BANDLIMIT}}(f-m/h) \ .$$

This can be rewritten as a convolution:

$$\widetilde{\text{SAMPLEWT}}(f) = \int_{-\infty}^{+\infty} df'\ \sum_m \delta(f-m/h-f')\ \widetilde{\text{EXACT}}(f')\ \widetilde{\text{BANDLIMIT}}(f')$$

$$= \int df'\ \widetilde{\text{SAMPLE}}(f-f')\ \widetilde{\text{EXACT}}(f')\ \widetilde{\text{BANDLIMIT}}(f') \ .$$

The Fourier transform of $\widetilde{\text{BANDLIMIT}}(f)$ is

$$\text{BANDLIMIT}(t) = \int_{-\infty}^{+\infty} df\ \widetilde{\text{BANDLIMIT}}(f)\ e^{-i2\pi ft}$$

$$= \int_{-1/2h}^{+1/2h} df\ e^{-i2\pi ft}$$

$$= \frac{\sin(\pi t/h)}{\pi t/h} .$$

The Fourier transform of $\widetilde{\text{EXACT}}(f)$ is given by the original definition of EXACT(t):

$$\text{EXACT}(t) = 1 \quad \text{if } |t| < L/2$$

$$= 1/2 \text{ if } |t| = L/2$$

$$= 0 \quad \text{if } |t| > L/2 .$$

Now apply the Fourier convolution theorem twice to the last formula for $\widetilde{\text{SAMPLEWT}}(f)$:

$$\text{SAMPLEWT}(t) = \text{SAMPLE}(t) \int_{-\infty}^{+\infty} dt'\ \text{EXACT}(t-t')\ \text{BANDLIMIT}(t')$$

$$= \sum_{k=-\infty}^{+\infty} h\ \delta(t-kh) \int_{t-L/2}^{t+L/2} dt'\ \frac{\sin(\pi t'/h)}{\pi t'/h}$$

$$= \sum_{k} \delta(t-kh)\ h\ \text{WT}(k), \text{ where}$$

$$\text{WT}(k) = \frac{1}{\pi}\ \text{Si}(\pi[k+N]) - \text{Si}(\pi[k-N]) , \text{ where}$$

$$\text{Si}(\Psi) \equiv \int_{-\infty}^{\Psi} d\Psi'\ \frac{\sin \Psi'}{\Psi'} \text{ and } N \equiv L/2h .$$

This last integral is reasonably well known [7]. The weights are particularly simple if $h << L$. The weights extend indefinitely far outside the integration domain, but they approach zero. In the center of integration domain they approach 1. Near either end, they oscillate about the trapezoidal weights. More precisely, suppose that k is not near either end: $\pi\,|k + N| >> 1$ and $\pi\,|k - N| >> 1$. Then the weights are approximately:

$$WT(k) \approx \frac{(-)^{k-N}}{\pi^2}\left[\frac{1}{k-N} - \frac{1}{k+N}\right] \text{ if } k \text{ is outside the domain}$$

$$\approx 1 - \frac{(-)^{k-N}}{\pi^2}\left[\frac{1}{k-N} - \frac{1}{k+N}\right] \text{ if } k \text{ is inside the domain.}$$

Near the end, a few weights are:

k - N	TRAP WT	CGG WT	NEW WT
+5	0	0	0 -.020,11
+4	0	0	0 +.025,03
+3	0	0	0 -.033,09
+2	0	0	0 +.048,59
+1	0	0 -.041,67	0 -.089,49
0	1/2	1/2	1/2
-1	1	1 +.041,67	1 +.089,49
-2	1	1	1 -.048,59
-3	1	1	1 +.033,09
-4	1	1	1 -.025,03
-5	1	1	1 +.020,11

This table assumes $|k - N| << N$. This rule is sketched in Fig. 4.

Our construction immediately tells us the Fourier error coefficient for this new rule:

$$\tilde{ENEW}(f) = \tilde{EXACT}(\text{mod}(f)) - \tilde{EXACT}(f)$$

$$= \frac{\sin(\pi fL)}{\pi\ \text{mod}(f)} - \frac{\sin(\pi fL)}{\pi f} .$$

This oscillates rapidly in f. As usual, it can be factored into a slowly changing modulation times the kernel of the rectangular rule:

$$\tilde{ENEW}(f) = \tilde{RECT}(f)\ \tilde{MODNEW}(f), \text{ where}$$

$$\tilde{MODNEW}(f) = \frac{\sin(\pi fh)}{\pi\ h\ \text{mod}(f)} - \frac{\sin(\pi fh)}{\pi fh} .$$

This is not singular since mod(f) and sin(πfh) have the same zeroes.

This new modulation is shown in Figs. 6ABC. Compare it with the other rules in those figures. The new rule is much better if $|f| < 1/2h$, since it has zero error. Thus this new rule is exact on "band-limited" functions which contain only these frequencies. For higher frequencies $|f| > 1/2h$, the new rule's errors are approximately comparable to the other rules.

What does this do for frequencies such that $\sin(\pi fL) = 0$? If f is an integer multiple of 1/L, but not an integer multiple of 1/h, then the error will be zero because $\widetilde{\text{RECT}}(f)$ is zero. At multiples of 1/h the error will not be zero because of aliasing.

Thus we have found a new rule which optimizes the mean square error spectrum: No other rule can have these zeroes and more. Notice that this same rule optimizes the maximum error bound and the exact error in the same way:

$$|\widetilde{\text{ENEW}}(f)|^2 = 0 \longleftrightarrow |\widetilde{\text{ENEW}}(f)| = 0 \longleftrightarrow \widetilde{\text{ENEW}}(f) = 0.$$

For a specific integrand with an approximately known power spectrum, we might do a little better. For example, if $|\widetilde{G}(f)|^2$ is known to be tuned to frequencies near f_1, then we should retune this rule by multiplying each weight WT(k) by $\exp(-2\pi f_1 kh)$. However, many integrands are large at low frequencies and fall off rapidly above some f_{max}. If it is possible to make h smaller than $1/f_{max}$, then even such specialized rules will show little improvement over the current one.

This new rule was derived from frequency arguments without explicitly studying polynomials. Therefore it is interesting that the same rule can be derived by fitting the same extended samples with a Lagrangian polynomial [1, p. 551] and then integrating that polynomial.

Notice that this new rule requires an infinitely extended data domain. This rule will be useful in either of several cases:

1) The integrand is known everywhere at $t = y+kh$.

2) The integrand gets small for large t, and the integrand is known far enough beyond the domain for the product of the weight and the integrand to become negligible.

3) The integrand is periodic, or approximately periodic. This period may be different from the integration domain.

In the last case, the preceding derivation must be slightly modified. The frequency f becomes discrete, and we must replace the factors

$$1/\pi f \quad \text{by} \quad L_{period}/\sin(\pi f L_{period}) \ .$$

These applications form a usefully large set. Unfortunately, sometimes the integrand is known only over a more limited data domain, or the integrand is large or irregular outside the integration domain. In those cases, the optimal rule is probably <u>not</u> to truncate the current one. There the optimum depends on the data domain. More work is needed.

CONCLUSIONS AND FUTURE WORK. What have we learned about numerical integration? What extensions follow? The first new idea in this paper was to study numerical integration as a function of the alignment of the samples. We found that numerical integration on $(-\infty, +\infty)$ was a periodic function of the alignment. This forced us to use the Fourier convolution theorem. The result was a family of error estimates based on the Fourier transform of the integrand. Sometimes these Fourier estimates were better than classical polynomial-derivative methods. Some of these Fourier errors were interpreted via Nyquist's theorem and the uncertainty principle. Other errors were due to extrapolation problems near the ends of the samples. One

improvement was higher order extrapolation near the ends. Simpson's rule did this in a clumsy way, which needlessly increased the Nyquist errors. A better solution was to use extended samples from beyond the integration domain. The Gauss-Gregory rule did this a little, and for many applications it is better than Simpson's rule. We found a new optimal rule which used a greatly extended data domain. It gave outstandingly small errors, which were interpreted via band-limited functions.

Several subsequent studies should be made. First, what is the optimal rule if the data domain does not extend infinitely? Second, a similar analysis can be based on autocorrelation. Let

$$\mathrm{AUTO}(G;y) \equiv \int dz\ G^*(y-z)\ G(z)$$

It follows that

$$||\mathrm{ERR}(G)||^2 = \int dy\ |\mathrm{ERR}(G;y)|^2 = \mathrm{AUTO}(G;0)$$
$$= \int dy\ \mathrm{AUTO}(\mathrm{SAMPLEWT}-1;y)\ \mathrm{AUTO}(G;-y)\ .$$

This last formula is like $||\mathrm{ERR}||^2 = \int df\ |\tilde{G}|^2\ |\tilde{E}|^2$.

A third direction is to study how other numerical analysis methods depend on the sample alignment. For example, suppose we evaluate a differential equation with a numerical integration scheme using equally spaced steps. How do the solutions change as the alignment changes?

There are several exciting new ideas which have more general interest. First, an ensemble of similar algorithms may be more fruitful to analyze than an individual algorithm. Second, an ensemble of exact calculations often has a group of symmetries. If an ensemble of algorithms are correct approximations to the exact calculations, then the group structure should be a powerful tool to analyze the algorithms. This should be applicable to many numerical analysis problems. These ideas are one step on a promising bridge between numerical analysis and group theory.

I am pleased to acknowledge important suggestions and critical reviews of this manuscript by Loren Meissner (Lawrence Berkeley Laboratory), Tsvi White (University of California, Berkeley) and Richard Hamming (Naval Postgraduate School, Monterey).

REFERENCES

1. R.W. Hamming, Numerical Methods for Scientists and Engineers, Second Edition, McGraw-Hill, New York, 1973. This has a very readable introduction to Fourier methods in numerical analysis.

2. E. Oran Brigham, The Fast Fourier Transform, Prentice Hall, Englewood Cliffs, N.J., 1973. This analysis benefitted from his clear development of the Fourier series as a limit of the Fourier integral, and his graphical technique to calculate with delta functionals.

3. A. Pappoulis, The Fourier Integral and Its Application, McGraw-Hill, New York, 1962, p. 44.

4. Leonard I. Schiff, Quantum Mechanics, Third Edition, McGraw-Hill, New York, 1968, pp. 60-62, pp. 187-234. This discusses the uncertainty principle and begins the broad subject of symmetries in quantum mechanics.

5. George Arfken, Mathematical Methods for Physicists, Second Edition, Academic Press, New York, 1970, pp. 278-283. This gives a good development of the Bernoulli numbers and the Euler-Maclaurin formula with a remainder term.

6. L.J. Comrie, Chambers' Six Figure Mathematical Tables, W.R. Chambers, London, 1959, pp. 546-549. This shows a variety of end corrections for numerical integration rules, including both closed and extended rules. See also [1., pp. 310-316].

7. E. Jahnke, F. Emde, F. Losch, Table of Functions, McGraw-Hill, New York, 1960, pp. 17-25. In addition to the relevant tables and approximations, the graphs here are a visual delight. See also M. Abramowitz and I.A. Stegun, Handbook of Mathematic Functions, National Bureau of Standards, Applied Mathematics Series 55, 1970, pp. 231-244.

APPENDIX A: CONVERGENCE. The following argument shows that the finite domain norm for $||\,ERR(G)\,||^2$ converges:

$$||\,ERR(G)\,||^2 \equiv \frac{1}{L}\int_{-\infty}^{+\infty} dy\ |\,ERR(G;y)\,|^2$$

$$= \frac{1}{L}\int_{-\infty}^{+\infty} dy\ \Big|\ \sum_{k=-\infty}^{+\infty} k\ WT(kh)\ G(y-kh) - \int_{-\infty}^{+\infty} dt\ EXACT(t)\ G(y-t)\Big|^2$$

$$= \sum_k \sum_{k'} h^2\ WT(kh)\ WT^*(k'h)\ \ \frac{1}{L}\int dy\ G(y-kh)\ G^*(y-k'h)$$

$$+ \int dt \int dt'\ EXACT(t)\ EXACT^*(t')\ \frac{1}{L}\int dy\ G(y-t)\ G^*(y-t')$$

$$+ \sum_k h \int dt'\ WT(kh)\ EXACT^*(t')\ \frac{1}{L}\int dy\ G(y-kh)\ G^*(y-t')$$

$$+ \int dt \sum_k h\ EXACT(t)\ WT(k'h)\ \frac{1}{L}\int dy\ G(y-t)\ G^*(y-k'h)$$

$$\leqslant \{\sum_k h\ |\,WT(kh)\,| + \int dt\ |\,EXACT(t)\,|\}^2\ \ \frac{1}{L}\int dt\ |\,G(t)\,|^2\ .$$

The discussion of numerical integration over the entire real line skated past some very pathological operators.

$$SAMPLE(y) = \sum_{k=-\infty}^{+\infty} h\ \delta(y-kh)\ .$$

A more rigorous approach would have been to first study numerical integration on a finite domain [-L/2; +L/2]. There SAMPLEWT(y) and $\widetilde{ERR}(G;f)$ are less pathological. After we had the Fourier decompositions for ERR(G;y) and MAX $|\,ERR(G;y)\,|$ and $||\,ERR(G)\,||^2$, then we could have taken the limit $L \to \infty$.

Unfortunately, this rearrangement would have many heuristic disadvantages. Numerical integration on a finite domain does not have the clear translation invariance that it does on the entire real line. Therefore, the finite domain case does not have the striking periodicity in y. Another disadvantage is the extrapolation problem. This reorganization would require us to analyze this complicated problem at the very beginning. I have balanced these advantages and disadvantages and chosen clarity over rigor; I hope that the reader agrees.

APPENDIX B: EVALUATION OF THE FOURIER TRANSFORMS. Here we will evaluate the Fourier transformation of four numerical integration rules. Each of these is a linear operator on the space of integrands. These operators are local with respect to t, and also are local with respect to f. The algebra of these local operators is like the algebra of functions of t or functions of f. We can formally write the effect of an operator on an integrand as a convolution between the integrand and a kernel. However, the kernel is not a well defined function, although it does represent a well defined operator. In this sense the sums of delta functionals, particularly SAMPLEWT and SAMPLE, are well defined.

The rectangular rule operator, and its Fourier transform are

$$\mathrm{RECT}(t) = \sum_{k=-n+1/2}^{+N-1/2} h\ \delta(t-kh)\ , \qquad \text{where } N \equiv 1/2h$$

$$\mathrm{RECT}(f) = \int_{-\infty}^{+\infty} dt\ \mathrm{RECT}(t)\ e^{+i2\pi ft} = \sum_k e^{+i2\pi fkh}$$

$$= h\ \sin(\pi fNh)/\sin(\pi fh)$$

Therefore the numerical integration error is

$$\widetilde{\mathrm{ERECT}}(f) \equiv \widetilde{\mathrm{RECT}}(f) - \widetilde{\mathrm{EXACT}}(f)$$

$$= \widetilde{\mathrm{RECT}}(f)\ [1 - \widetilde{\mathrm{EXACT}}(f) / \widetilde{\mathrm{RECT}}(f)]$$

$$= \widetilde{\mathrm{RECT}}(f)\ [1 - \sin(\pi fh) / \pi fh]$$

Hereafter use $\theta \equiv \pi fh$.

The trapezoidal rule operator is

$$\mathrm{TRAP}(t) = \frac{h}{2}\ \delta(t-L/2) + \sum_{k=-N+1}^{+N-1} h\ \delta(t-kh) + \frac{h}{2}\ \delta(t + L/2)\ .$$

The trapezoidal rule is the average of two rectangular rules, each shifted $\pm h/2$. This can be expressed by convolution (i.e., composition of linear operators). Then the Fourier transform of TRAP will easily follow by the Fourier convolution theorem:

$$\text{TRAP}(t) = \int_{-\infty}^{+\infty} dt' \; \text{RECT}(t-t') \; \text{WTRAP}(t') \;, \quad \text{where}$$

$$\text{WTRAP}(t') \equiv 1/2 \; \delta(t' - h/2) + 1/2 \; \delta(t' + h/2),$$

whose Fourier transform is

$$\widetilde{\text{WTRAP}}(f) = 1/2 \; e^{-i2\pi fh/2} + 1/2 \; e^{+i2\pi fh/2} = \cos\theta$$

$$\therefore \widetilde{\text{TRAP}}(f) = \widetilde{\text{RECT}}(f) \cos\theta$$

Therefore the corresponding error operator is

$$\widetilde{\text{ETRAP}}(f) = \widetilde{\text{TRAP}}(f) - \widetilde{\text{EXACT}}(f)$$

$$= \widetilde{\text{RECT}}(f) \; [\cos\theta - \sin\theta/\theta]$$

The operator for Simpson's rule is

$$\text{SIMP}(t) = \frac{h}{3} \delta(t-L/2) + \frac{4}{3} \sum_{\substack{\text{even } k \\ |k| < N}} h \quad (t-kh)$$

$$+ \frac{2}{3} \sum_{\substack{\text{odd } k \\ |k| < N}} h \; \delta(t-kh) + \frac{h}{3} \delta(t+L/2) \; .$$

Observe the sum of vectors

$$\begin{array}{ccccccc} 1 & 0 & 1 & 0 & 1 & 0 & 0 \\ 0 & 4 & 0 & 4 & 0 & 4 & 0 \\ 0 & 0 & 1 & 0 & 1 & 0 & 1 \\ \hline 1 & 4 & 2 & 4 & 2 & 4 & 1 \end{array} \; .$$

This generates the pattern of weights for Simpson's rule. Thus Simpson's rule is the weighted average of three shifted operators. Each operator is like the rectangular rule, but with half the density of samples:

$$\text{RECT2H}(t) \equiv \sum_{k=-N/2+1/2}^{+N/2-1/2} 2h\ \delta(t-2hk)$$

$$\text{WSIMP}(t') \equiv \frac{1}{6}\delta(t'-h) + \frac{4}{6}\delta(t') + \frac{1}{6}\delta(t'+h)$$

$$\text{SIMP}(t) = \int_{-\infty}^{+\infty} dt'\ \text{RECT2H}(t-t')\ \text{WSIMP}(t')$$

$$\widetilde{\text{SIMP}}(f) = \widetilde{\text{RECT2H}}(f)\ \widetilde{\text{WSIMP}}(f), \quad \text{where}$$

$$\widetilde{\text{RECT2H}}(f) = 2h\ \sin(\pi f \times \frac{N}{2} \times 2h)\ /\ \sin(\pi f \times 2h)$$

$$\widetilde{\text{WSIMP}}(f) = \frac{1}{6}\, e^{-i2\pi fh} + \frac{4}{6} + \frac{1}{6}\, e^{-i2\pi fh}$$

$$= \frac{2}{3} + \frac{1}{3}\cos(2\pi fh) \ .$$

Therefore the error is

$$\widetilde{\text{ESIMP}}(f) = \widetilde{\text{RECT2H}}(f) - \widetilde{\text{EXACT}}(f)$$

$$= \widetilde{\text{RECT2H}}(f)\ [\frac{2}{3} + \frac{1}{3}\cos(2\theta) - \sin(2\theta)/2\theta] \ .$$

The centered first order Gauss-Gregory rule corrects the trapezoidal rule with centered differences at each end:

$$\text{CGG} \equiv \text{TRAP}(t) + \text{CORRECTION}(t)$$

$$\text{CORRECTION}(t) = \frac{h}{24}\ [\delta(+L/2+h-t) - \delta(+L/2-h-t) + \delta(-L/2-h-t) + \delta(-L/2+h-t)] \ .$$

From the preceding description, it is reasonable to analyze the correction operator as a composition of two other operators:

$$\text{CENTERED DIFFERENCE}(t) \equiv \frac{1}{2}\delta(h-t) - \frac{1}{2}\delta(-h-t)$$

$$\text{AT EACH END}(t) \equiv +\delta(L-t) - \delta(-L-t)$$

$$\text{CORRECTION}(t) = -\frac{h}{12}\int dt'\ \text{CENTERED DIFFERENCE}(t-t')\ \text{AT EACH END}(t')$$

$$\widetilde{\text{CORRECTION}}(f) = -\frac{h}{12} \times 2i\ \sin(\pi fh) \times 2i\ \sin(\pi fL)$$

$$= \frac{1}{3}\sin^2(\pi fh)\ \widetilde{\text{RECT}}(f) \ .$$

Therefore the error is

$$\begin{aligned}\widetilde{ECGG}(f) &\equiv \widetilde{CGG}(f) - \widetilde{EXACT}(f) \\ &= \widetilde{TRAP}(f) + \widetilde{CORRECTION}(f) - \widetilde{EXACT}(f) \\ &= \widetilde{RECT}(f)\ [\cos\theta + \tfrac{1}{3}\sin^2\theta - \sin\theta/\theta]\ .\end{aligned}$$

FIGURE CAPTIONS

Fig. 1AB. These two graphs show two numerical integrals which approximate the same exact integral. Each arrow represents a sample G(y+kh). Compare the samples; the alignment y is different, so the samples are shifted between the two. In order to make the numerical integration errors more visible (in Fig. 2B), in Figs. 1AB and 2AB I show a very coarse numerical integration, and use the square of a Breit-Wigner as the integrand. This is slightly different from the case discussed in the introduction.

Fig. 2AB. These graphically illustrate the calculation of the numerical integral NI(G;y) and some of its properties. In Fig. 2A we repeat the integrand and the sample arrows from Fig. 1, but with offsets $\Delta y = kh$. The result is that the sample arrows are superimposed at $y = 0$. The numerical integral is the sum of these sample arrows. They are added graphically in Fig. 2B, to form NI(G;y=0). The other arrows show another numerical integral NI(G;y=h/2), with a different alignment. This corresponds to the samples shown in Fig. 1B. In Fig. 2B, the oscillating line at the top is NI(G;y), and the straight line is the exact integral. Notice that the numerical integral is periodic, has the right average value, and sometimes equals the exact integral.

Fig. 3. The exact integral and the numerical integral should be realigned together.

Fig. 4. A pictorial catalogue of numerical integration rules. Discrete sample operators are represented by arrows, whose lengths are the weights. The rectangular rule has uniform weights. The trapezoidal rule uses half-weighted samples at each end. Simpson's rule oscillates. The centered Gauss-Gregory (CGG) rule corrects the trapezoidal rule near the ends. It uses samples just beyond the ends of the integration domain. The new, optimal rule uses samples far beyond the ends, but with decreasing weights. These weights oscillate around the trapezoidal rule. The sketch exaggerates this oscillation by 2:1 to make it more visible.

Fig. 5AB. The Fourier transform of the rectangular rule $\widetilde{\text{RECT}}(f)$ is shown in Fig. 5A. Notice the large Nyquist spikes at harmonics of the sampling frequency 1 cycle/sample = 1/h. The modulation MODRECT(f) is the smooth curve in Fig. 5B. The oscillating curve is the error coefficient ERECT(f), which is the product of RECT(f) and MODRECT(f).

Fig. 6ABC. These graphs show the absolute values of the different modulations. The smallest modulation will have the smallest error coefficient. Figure 6A shows the low and intermediate frequency band $0 \leq f \leq 1.0$ cycle/sample. Figures 6B and 6C go to higher frequencies $0 \leq f \leq 3$ cycles/sample. Figure 6B shows the individual curves, but with a consistent overall scale. Figure 6C superimposes them for comparison. These figures are discussed in detail in the main text.

Fig. 7ABC. These show the error coefficients for Simpson's rule $\widetilde{ESIMP}(f)$ (Fig. 7A), and for the centered Gauss-Gregory rule $\widetilde{ECGG}(f)$ (Fig. 7B), and for the new optimal rule $\widetilde{ENEW}(f)$ (Fig. 7C). Notice that Simpson's rule has double the density of large Nyquist spikes, compared to the other rules. These additional spikes in Fig. 7A have negative phase. In contrast, the new rule has exactly zero errors in the band up to $f = 1/2h$. Many integrands have most power at low frequencies (i.e.: $|\widetilde{G}(f)|^2$ is largest at low frequencies) so that this low frequency band is heavily weighted in the overall error.

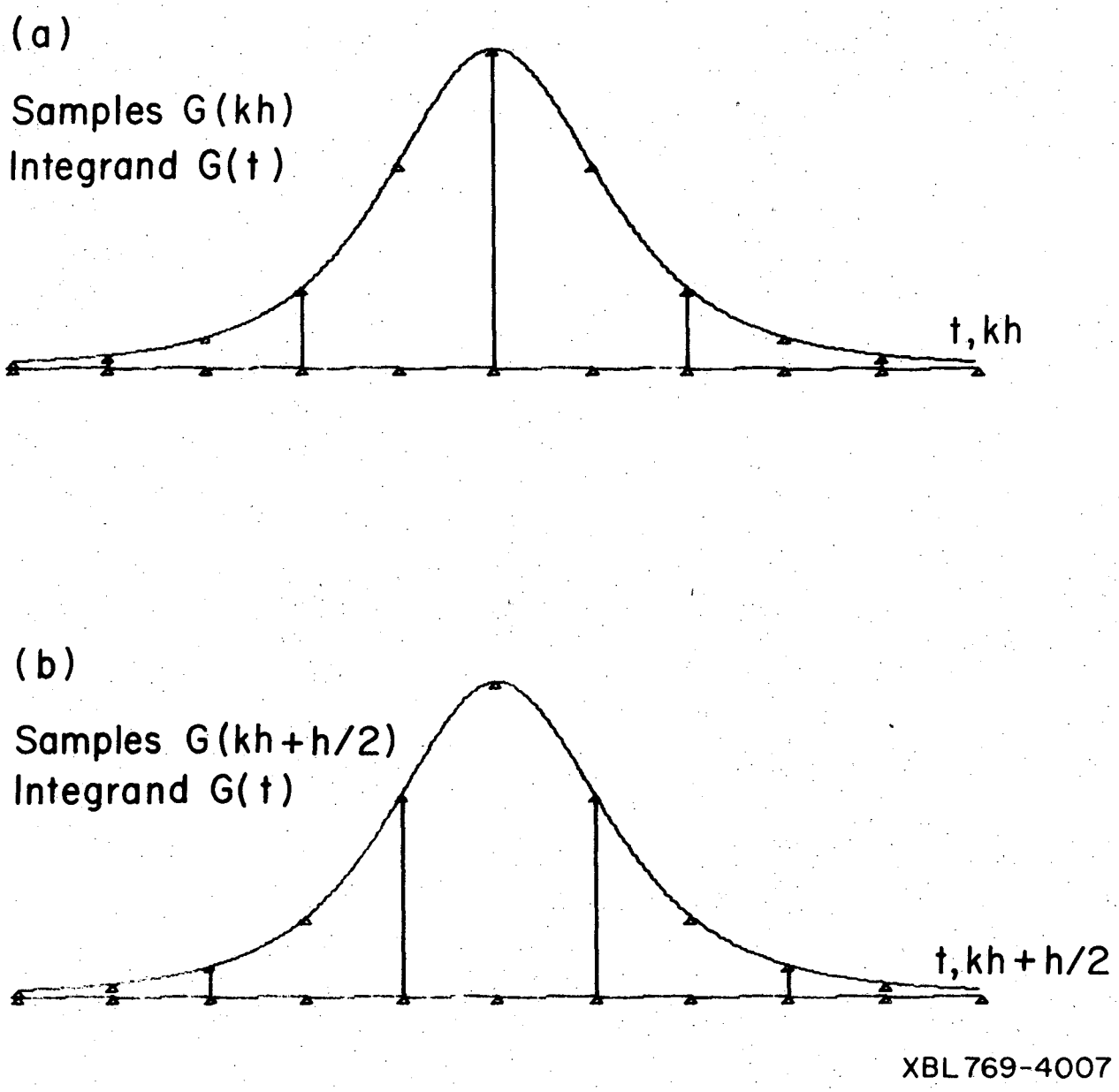
(a)
Samples G(kh)
Integrand G(t)
t, kh
(b)
Samples G(kh+h/2)
Integrand G(t)
t, kh+h/2
XBL769-4007

Fig. 1AB.

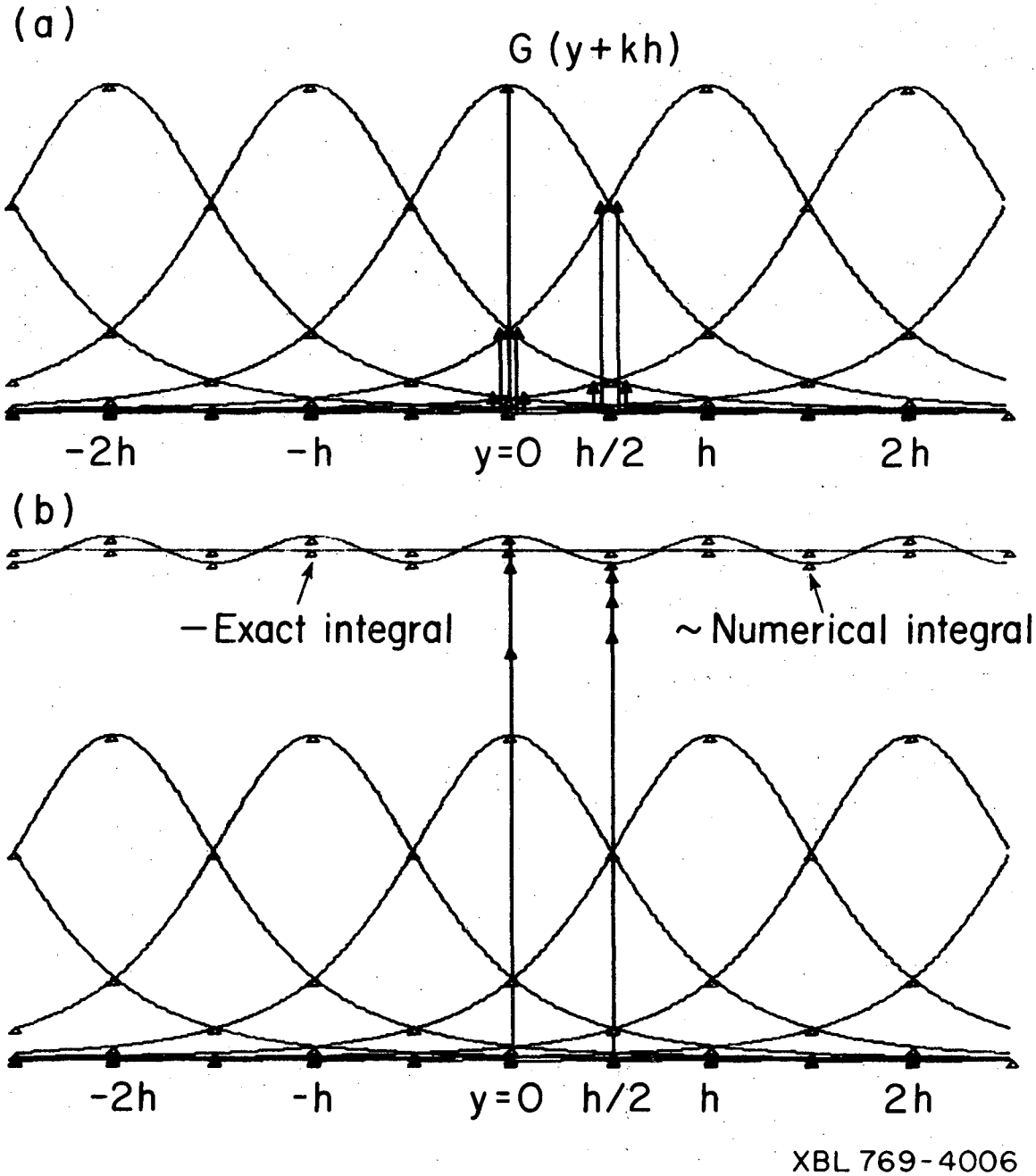

Fig. 2AB.

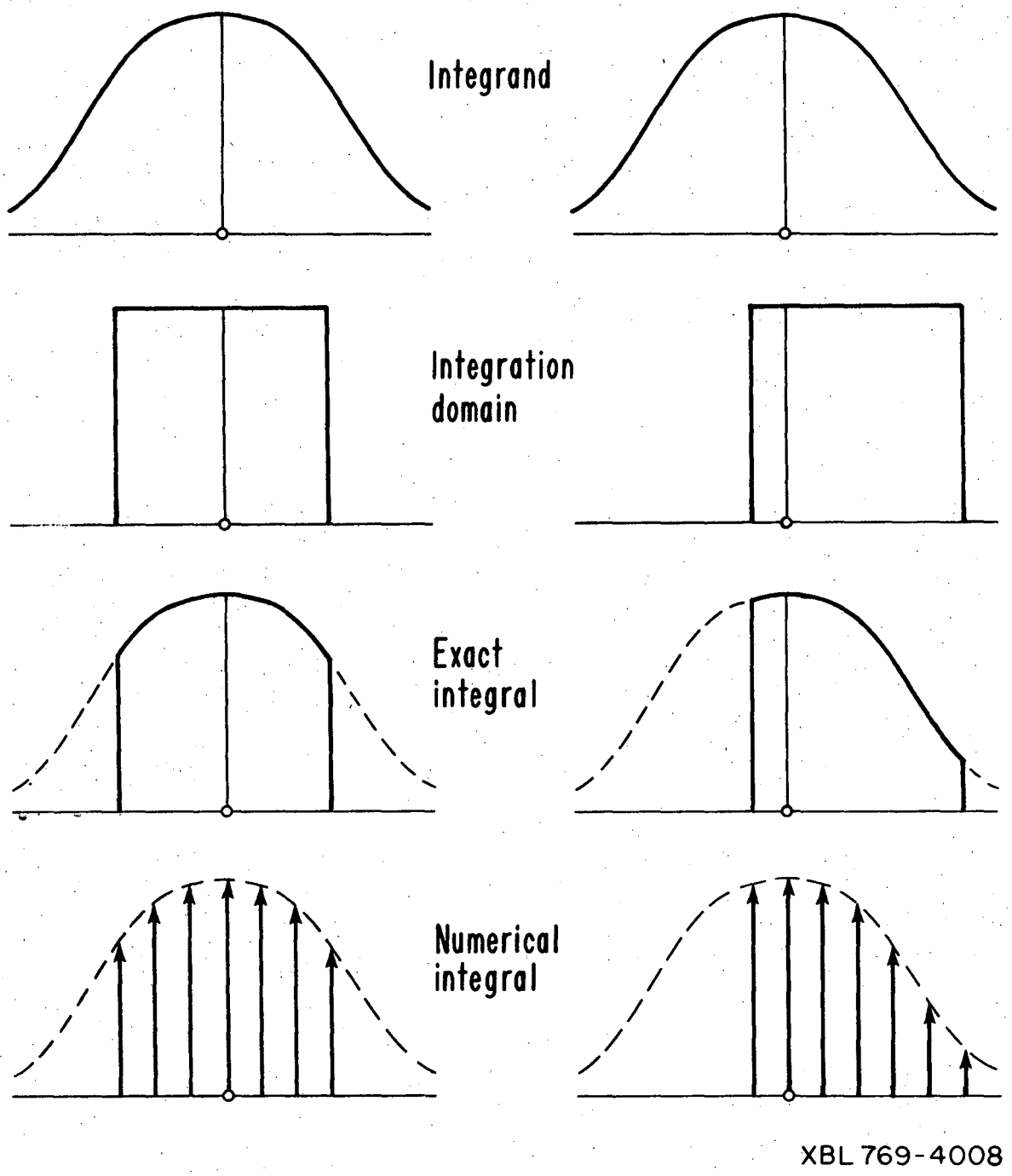
Integrand
Integration domain
Exact integral
Numerical integral
XBL 769-4008

Fig. 3.

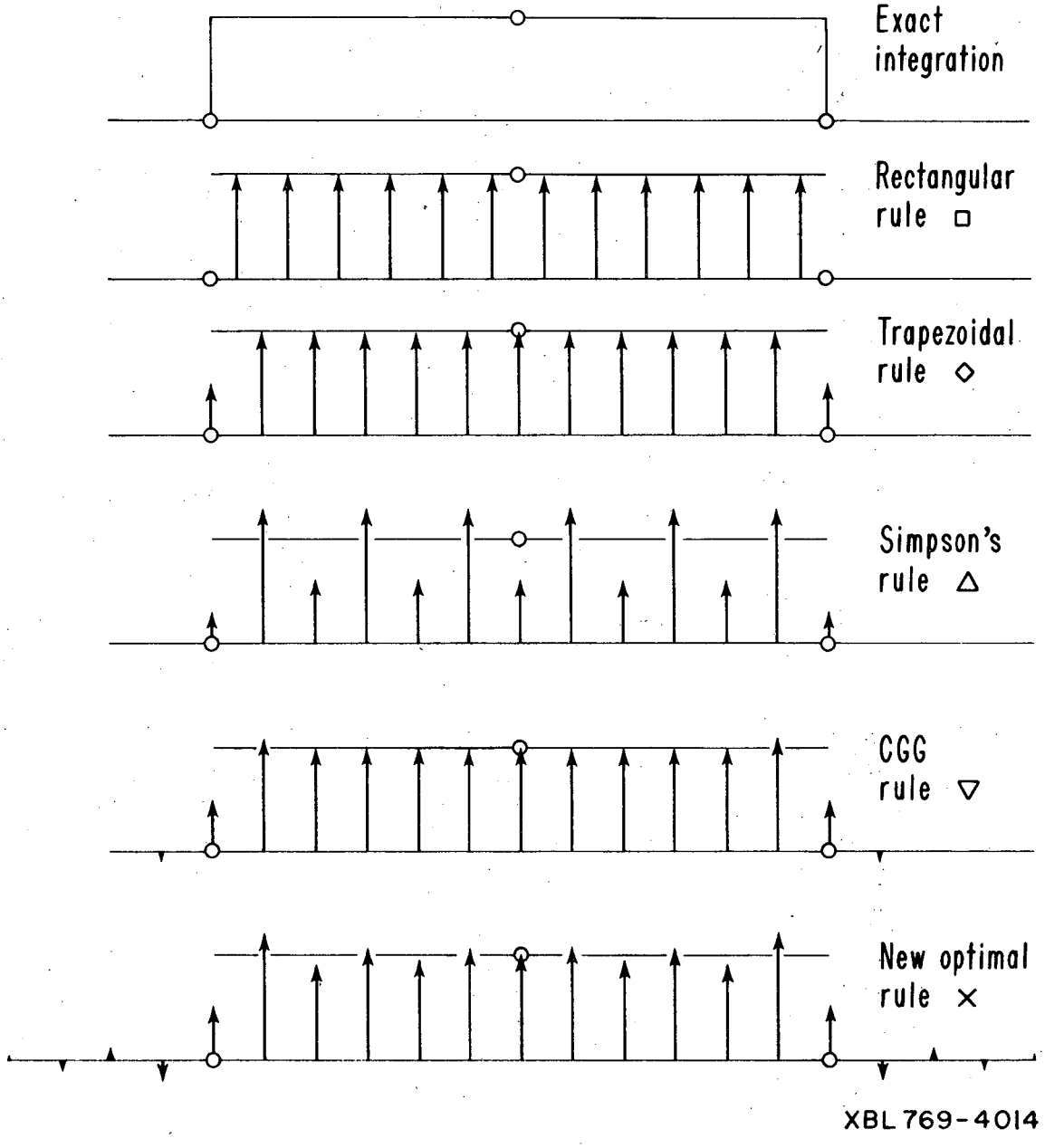

Fig. 4.

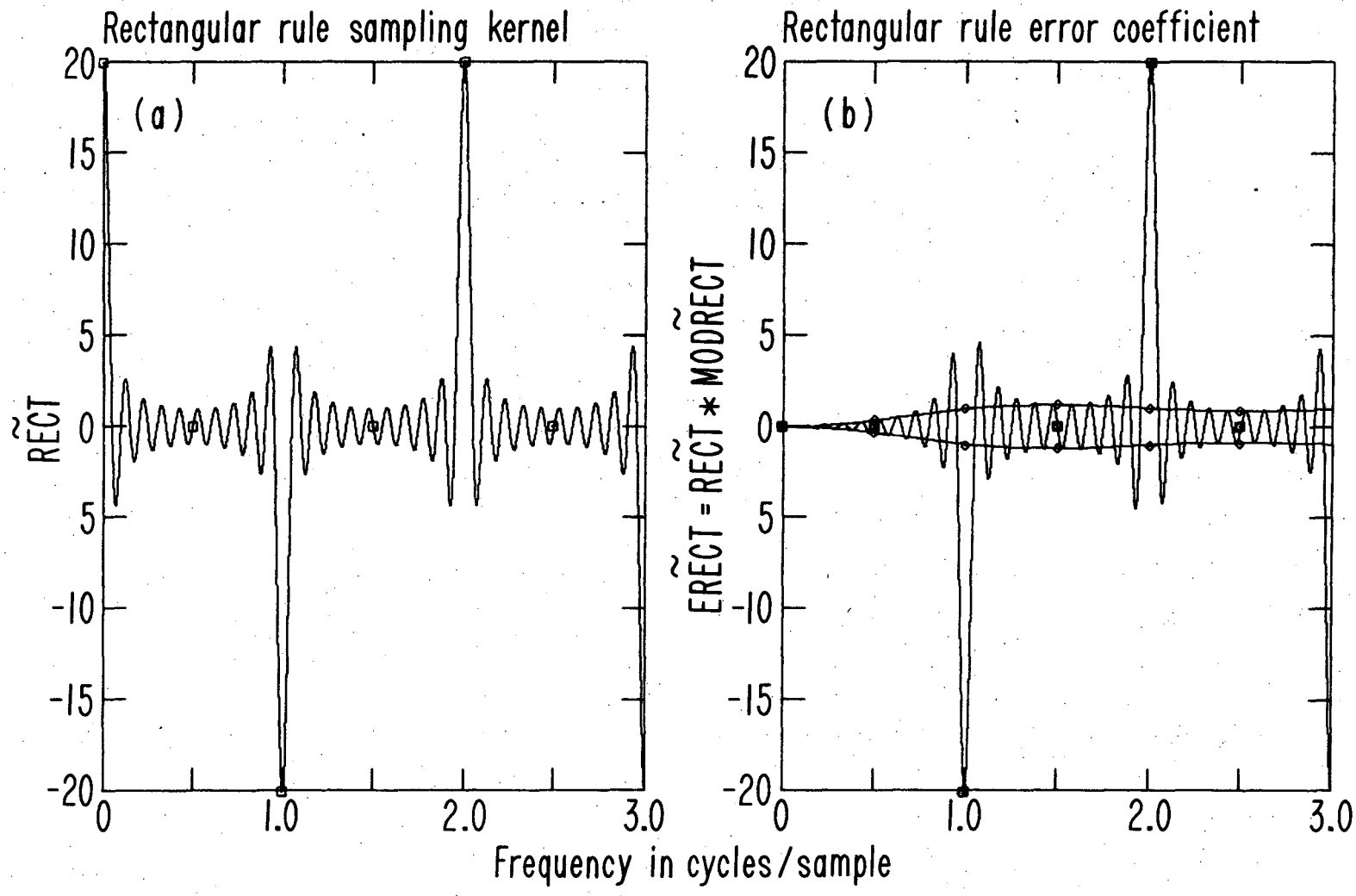

Fig. 5AB.

XBL769-4009

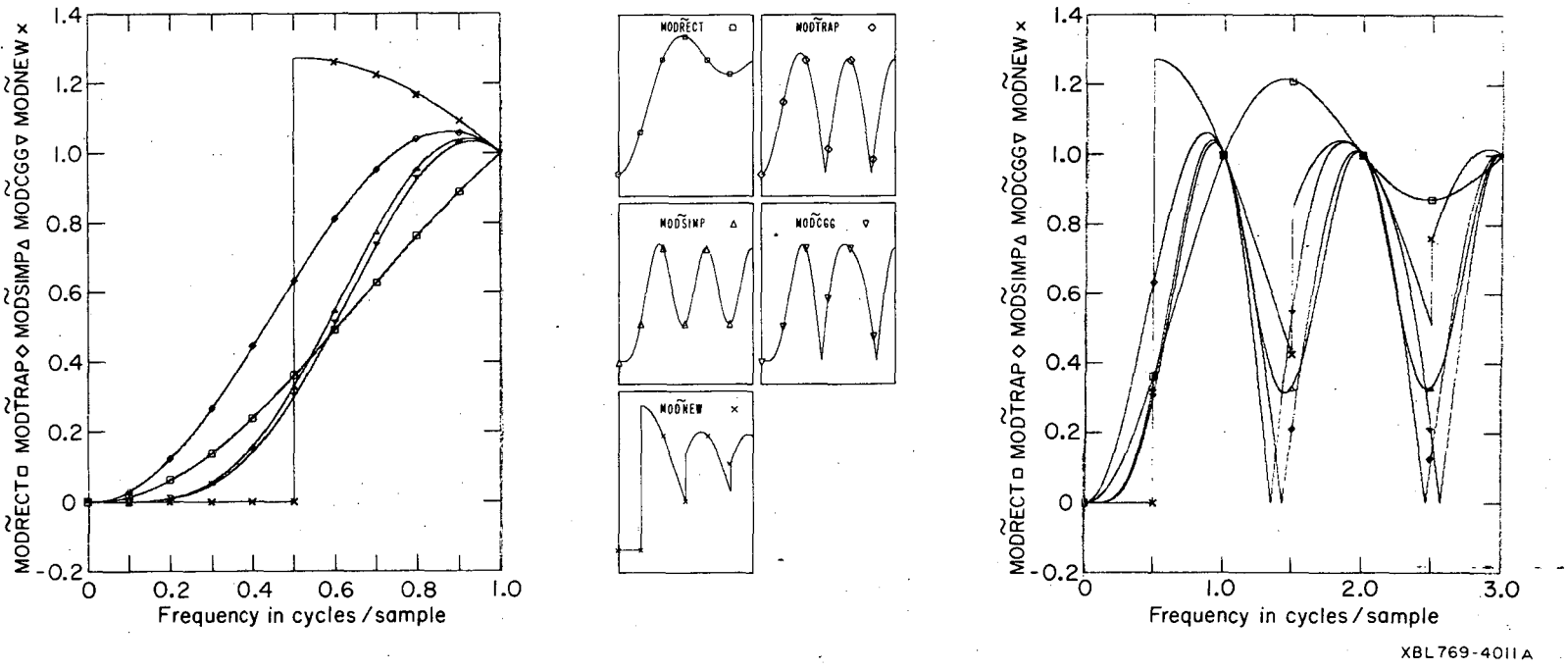
MODRECT □ MODTRAP ◇ MODSIMP △ MODCGG ▽ MODNEW ×
1.4
1.2
1.0
0.8
0.6
0.4
0.2
0
-0.2
0
0.2
0.4
0.6
0.8
1.0
Frequency in cycles / sample
MODRECT □
MODTRAP ◇
MODSIMP △
MODCGG ▽
MODNEW ×
1.4
1.2
1.0
0.8
0.6
0.4
0.2
0
-0.2
0
1.0
2.0
3.0
Frequency in cycles / sample
XBL769-4011A

Fig. 6ABC.

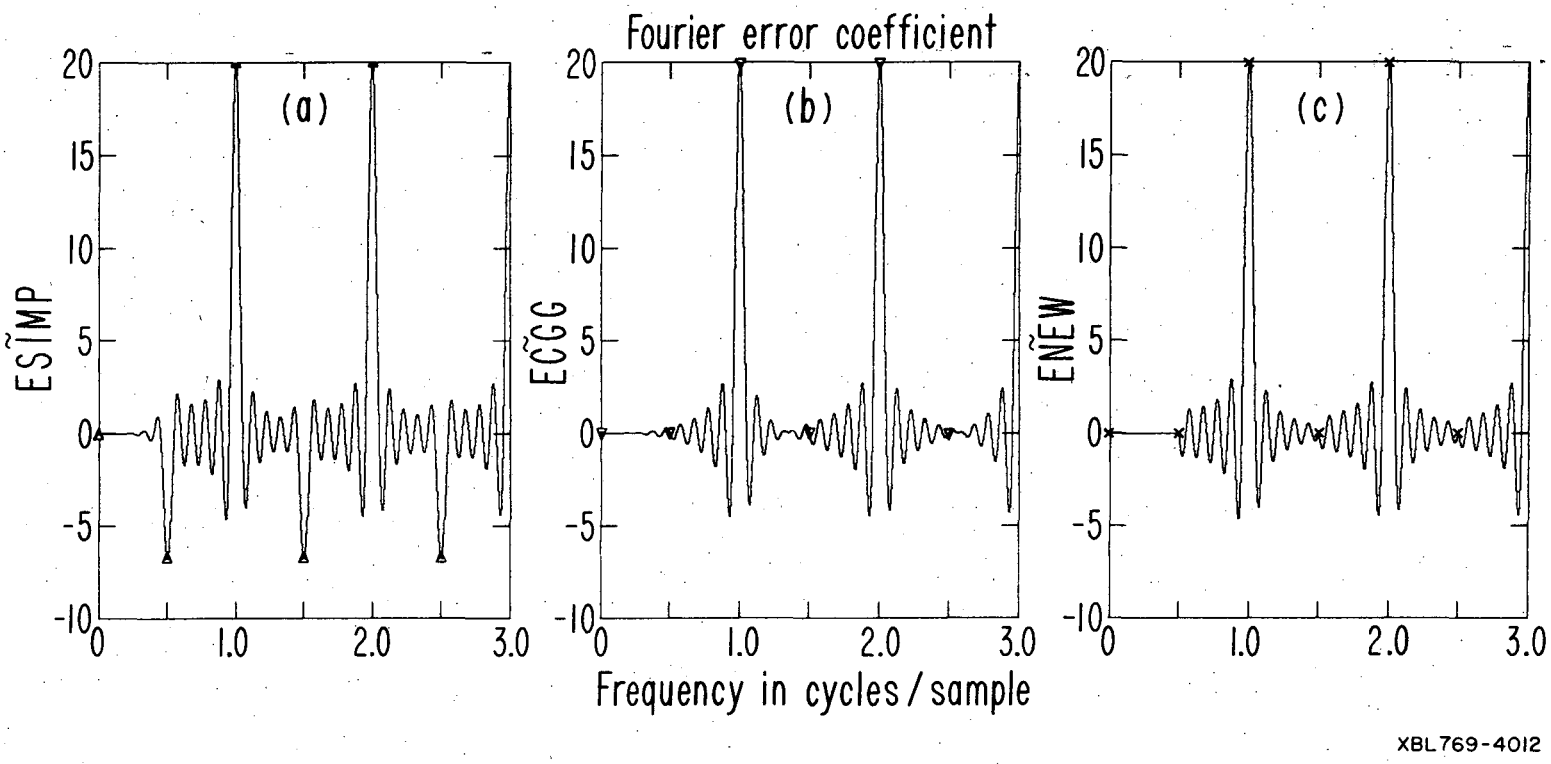
Fourier error coefficient
(a)
(b)
(c)
ESIMP
ECGG
ENEW
20
15
10
5
0
-5
-10
0
1.0
2.0
3.0
Frequency in cycles / sample
XBL769-4012

Fig. 7ABC.

This report was done with support from the United States Energy Research and Development Administration. Any conclusions or opinions expressed in this report represent solely those of the author(s) and not necessarily those of The Regents of the University of California, the Lawrence Berkeley Laboratory or the United States Energy Research and Development Administration.

TECHNICAL INFORMATION DIVISION
LAWRENCE BERKELEY LABORATORY
UNIVERSITY OF CALIFORNIA
BERKELEY, CALIFORNIA 94720